University of Thessaly

School of engineering

Department of Mechanical engineering

FLOW THROUGH FLEXIBLE PIPES IN HUMAN RESPIRATORY SYSTEM

Konstantinos Kyriakos

Nikolaos Vlastos

Volos, January 2020

This thesis is submitted for the partial fulfillment of the requirements for the Degree of Diploma in Mechanical Engineering

Certified by the members of the Thesis Committee:

1st Member: Dr. Bontozoglou Vassilios

(Supervisor) Professor, Department of Mechanical Engineering

University of Thessaly

2nd Member: Dr. Andritsos Nikolaos

Professor, Department of Mechanical Engineering

University of Thessaly

3rd Member: Dr. Valougeorgis Dimitrios

Professor, Department of Mechanical Engineering

University of Thessaly

Acknowledgments

We would like to express our gratitude to Dr. Bontozoglou Vassilios for his patience and guidance he showed in this thesis. Our collaboration was expectably interesting as we always appreciated his talent and passion in teaching. Without his support this thesis would have not been produced and we feel honored we worked together.

Moreover, we would like to thank the members of the thesis committee i.e. Dr. Andritsos Nikolaos and Dr. Valougeorgis Dimitrios, for the time they spent to examine our thesis and evaluate our research.

Περίληψη

Η ροή ενός ρευστού μέσα σε έναν αγωγό με ελαστική συμπεριφορά εμφανίζεται σε ένα ευρύ φάσμα βιομηχανικών αλλά και βιολογικών εφαρμογών. Το ανθρώπινο σώμα εντάσσεται στην τελευταία κατηγορία καθώς αποτελείται από πολλούς ελαστικούς αγωγούς . Στην παρούσα διπλωματική εξετάζουμε την διαδικασία αναπνοής συνδυάζοντας την θεωρητική ανάλυση με ένα υπολογιστικό μοντέλο το οποίο προβλέπει την συμπεριφορά ενός τυπικού ελαστικού αεραγωγού ο οποίος βρίσκεται μέσα στους πνεύμονες σε διαφορετικές καταστάσεις. Η έρευνα μας επικεντρώνεται, κυρίως, στο φαινόμενο της βεβιασμένης εκπνοής (forced expiration) το οποίο παρουσιάζει κάποια ενδιαφέροντα και σύνθετα αποτελέσματα που προσπαθήσαμε να ερμηνεύσουμε.

Αρχικά, περιγράψαμε κάποιες από τις εφαρμογές όπου χρησιμοποιούνται ελαστικοί σωλήνες και αναπτύξαμε τις βασικές εξισώσεις που περιγράφουν την κατάσταση των σωλήνων χρησιμοποιώντας έννοιες από την μηχανική των υλικών. Μετά από αυτήν την γενική προσέγγιση, εστιάζουμε στην περίπτωση του ανθρώπινου πνεύμονα ο οποίος αποτελείται από ένα δίκτυο κυλινδρικών αεραγωγών. Έπειτα, παρουσιάζεται μια σύντομη σύνοψη του ανθρώπινου πνεύμονα και των ελαστικών ιδιοτήτων του και στην συνέχεια εφαρμόζεται ένα απλοποιημένο μοντέλο που υπάρχει στην βιβλιογραφία κατασκευάζοντας το από την αρχή βασισμένοι στους θεμελιώδεις νόμους της ρευστομηχανικής. Το μοντέλο αναφέρεται σε ροή ενός σωλήνα και πραγματοποιούνται οι παραδοχές της μονοδιάστατης, ψευδο-μόνιμης και ασυμπίεστης ροής. Οι υπολογισμοί εκτελούνται μέσω της Fortran και τα αποτελέσματα που λήφθηκαν παρουσιάζονται σε διάφορες καμπύλες παροχής-πτώση πίεσης.

Τέλος, η ανάλυση οδηγείται στην διερεύνησή του φαινόμενου του περιορισμού της ροής (flow limitation) κατά την διάρκεια της βεβιασμένης εκπνοής το οποίο συμβαίνει στην περίπτωση που η ταχύτητα του αέρα προσεγγίζει την ταχύτητα διάδοσης του ελαστικού κύματος. Από τον λεπτομερή υπολογισμό που πραγματοποιήθηκε για την μεταβολή της πίεσης κατά μήκος του αγωγού, αποδείχθηκε ότι το συγκεκριμένο μοντέλο καθίσταται ανακριβές για να το αποτυπώσει. Οι πιθανές τροποποιήσεις που μπορούν να συμπεριληφθούν μελλοντικά για την ακριβέστερη προσέγγιση του προβλήματος είναι (i) η αποκόλληση της ροής στο σημείο της μέγιστης στένωσης (περιοχή λαιμού) που οδηγεί σε ανομοιομορφία στη διατομή ροής (σχηματισμός δέσμης και ανακυκλοφοριών) (ii) μη-μόνιμα φαινόμενα όπως η ταλάντωση του τοιχώματος και (iii) η κατάρρευση της κυκλικής διατομής.

Abstract

The flow of a fluid throughout a pipe with elastic behavior is involved in a wide range of industrial applications and biological systems. The human body is one of the latter as it consists of many elastic tubes. This thesis examines the breathing procedure, combining a theoretical analysis of the phenomenon with a computational model which predicts the behavior of a typical lung airway for different inflation states. Our research has been, mainly, focused on the problem of forced expiration which presents some interesting and complicated results that we tried to interpret.

At the beginning, we outline some of the applications of elastic pipes and construct the basic equations that describe the state of tubes in different cases using the concepts of material mechanics. After this general approach we specialize in the case of the human lung which consists of a complicated network of cylindrical airways. A brief synopsis of the human lung and its elastic properties is presented and then we implement a simplified model from the literature starting from the fundamental laws of fluid mechanics. The model simulates the flow through a single airway of a lung, assuming one dimensional, quasi-steady and incompressible flow. The computations were performed using Fortran and the results we received are presented in several curves of flow rate as a function of pressure drop.

The investigation focused on the phenomenon of “flow limitation” during forced expiration, which is associated with the singular behavior that occurs when air velocity approaches the propagation speed of elastic waves on the wall. By detailed computation of the variation of pressure along the airway, it was shown that the steady, one-dimensional model becomes inaccurate. Potential modifications, to be included in the model in future work, are (i) flow separation at the location of maximum constriction that results in jet flow, (ii) time-dependent phenomena such as wall fluttering and (iii) collapse of cross-section area.

Contents

List of Figures

List of Tables

1. Introduction-Applications

Transportation of fluids is an everyday phenomenon that exists in nature and engineering. Fluid dynamics is a subcategory of fluid mechanics that describes the flow of fluids (liquids and gases). To achieve this fluid flow or the transportation from one point to another it is necessary to form a path for it. The most common way is to use tubes with a round cross-section but are not the only ones. Rectangular, square, triangle or elliptical shapes are also used depending on the application each time.

Figure 1.1: Variety of rigid and deformable tubes with different cross-sectional area

Except from the different shapes of cross-sectional area, tubes can be divided more extensively into deformable and non-deformable, based on their construction material (significance level of deformation that takes place). There are these called non elastic-non deformable tubes in which the tube wall is rigid and deformation is negligible. Can be found at plenty applications such as in cooling or heating systems, in distribution of water at household units or at internal combustion engines. On the other hand, flexible tubes, which will be the type of tubes this analysis will examine, can be found in a wide range of applications as in oil and gas industries till biomechanics and biological systems.

In the following paragraphs, we choose some of the endless applications of flexible tubes that we find interesting and are worth to be mentioned.

Applications

Oil and gas industries use flexible tubes to transport the fluid from high pressure or high temperature environments to sea surface, if it's offshore (off land), or at the earth surface, if it's onshore (on land) *(Qiang Bai, Yong Bai, Ruan,2017)* . They can be applied in water depths up to 2.400 m., pressures up to 680 atm, high temperatures above 65,5 °C and can resist large vessel motions whenever the weather conditions are difficult. Flexible pipes which are used in these kinds of applications are classified into two categories based on the operating pressure and the reinforcement material: metal based and composite based flexible pipes *(Qiang Bai, Yong Bai, Ruan,2017)*. Metal based flexible pipes are designed to withstand high loads such as high internal, external pressure or large axial tension. Oppositely, composite based flexible pipes, also called FCP (Flexible Composite Pipes), have a more simple structure from metal based pipes and lower functional requirements. Both categories can be divided further in two groups based on their construction: bonded or unbonded. The difference between them is the existence of a flexible polymer matrix, usually an elastomer which contains the reinforcement. So, in bonded tubes the reinforcement is embedded at this polymer matrix while at the unbonded is independent of the matrix.

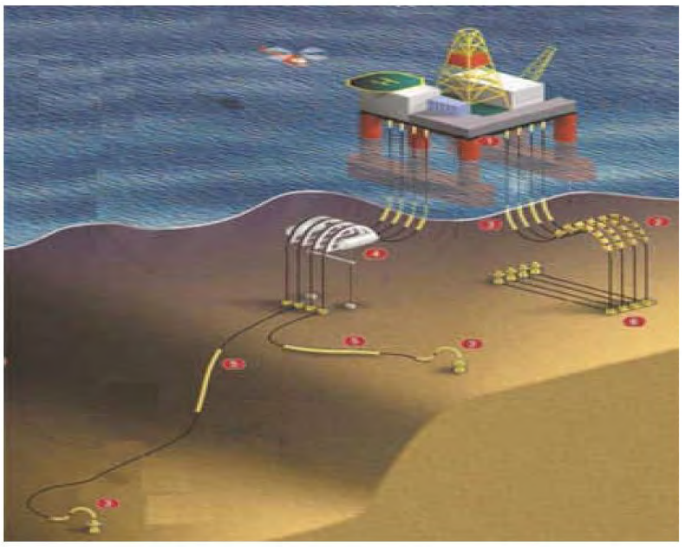

Figure 1.2: Offshore gas industry in which flexible pipes are used

Flexible tubes can be found, also, in a specific category of pumps called peristaltic pumps *(*https://en.wikipedia.org/wiki/Peristaltic_pump*)*. At first, pumps are devices that are used widely in

applications which contain fluid transfer and are responsible for providing extra energy to the fluid in order to complete this transportation. Depending on the operating principle that follow they can be divided into categories. Peristaltic pump belongs to positive displacement which means that the fluid volume is enclosed and moves mechanically through the system until the discharge pipe. This enclosure is achieved because the fluid is trapped between the pump's motor head (rotor) and the stationary area of the pump (stator). Specifically in peristaltic pump, the fluid passes through the flexible tube, and then the rotor's head, which can be "rollers", "shoes", "wipers" or "lobes", increases the external pressure causing the partial compression of the fluid inside. As the rotor turns, the part of tube which is under compression collapses and the fluid moves with the motion of rotor, through the tube, until the discharge pipe. Most commonly they are used to pump clean/sterile or aggressive fluids (are referred to these fluids which react with the surrounding materials). For example:

- Are applied in heart-lung machines to circulate blood during a bypass surgery.
- In hemodialysis systems which help removing excess water, solutes and toxins from the blood.
- Pumping aggressive chemicals, high solids slurries and other materials where they should not come into contact with the environment.
- The rollers of peristaltic pumps are suited for abrasive and high viscosity fluids. So, there are used in agriculture as they are well constructed for pumping agricultural chemicals.

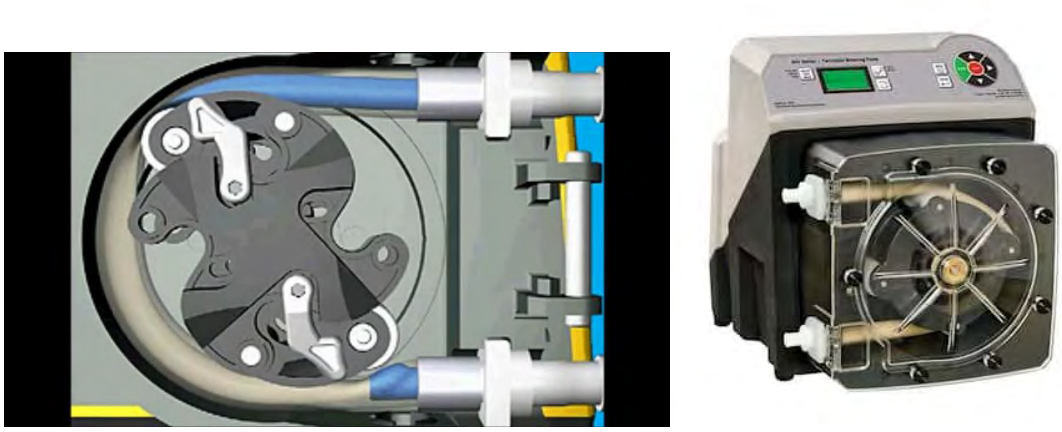

Figure 1.3: Inside view of peristaltic pump

Moreover, an important tool that used widely in medicine and presents elastic behavior is catheter. Catheters are thin deformable tubes which are inserted into the human body in order to treat diseases or perform surgical procedures. It has been discovered that the earliest invention of catheter was 3000 years ago from Syrians and it's use was to relieve them from urinary retention

*(*https://www.urotoday.com/urinary-catheters-home/history-of-urinary-catheters.html*)*. In those times Syrians were using straws, palm leaves, hollow top of onions as well as gold, silver, copper, brass and lead to construct a hollow catheter. The first flexible catheters were developed in the 11th century using as basic material silver because it could be formatted in different shapes and were considered that have an antiseptic action. Much later, during 18th century, Benjamin Franklin designed a more modern catheter to help his brother, who suffered from bladder stones. He constructed a catheter of silver metal with segments, hinged together with a wire enclosed to provide rigidity during insertion. Nowadays, catheters, *Figure 1.4*, are thin flexible tubes which can be made from a range of polymers such as silicone rubber, nylon, polyurethane, latex and thermoplastic elastomers. Depending on the operation, stiffness and size of catheters differ and they can be, either temporarily or permanently, inside the human body. Inserting a catheter into the body allows:

- Urinary catherization in which urine is draining from the urinary bladder via urethra checking, this way, the condition of the bladder.
- Drainage of air at the pleural space between lung and chest wall (pneumothorax) which causes chest pain and shortness of breath.
- To widen narrowed or obstructed arteries or veins (angioplasty) with the inflation of a balloon that is attached to the catheter (balloon catheter) inside the body and a stent to ensure that the vessel remains open.
- Measurement of blood pressure when it is important to define quickly changes of blood pressure.

  This is accomplished with the insertion of a catheter into the artery or vein which is connected with a pressure transducer. Otherwise, in normal conditions sphygmomanometer is used.

Figure 1.4: A modern typical Catheter

In agriculture and specifically, at low cost drip-irrigation systems where low pumping power is needed an innovative device of a deformable tube called ‘’Starling Resistor’’ *(Wang, Ruo-Qian, Teresa Lin, Pulkit Shamshery, Amos G. Winter,2016, http://hdl.handle.net/1721.1/109244)* can be applied. Before explaining it in more detail, it is crucial to understand the operation of drip irrigation in order to find out which type of water distributor can Starling resistor replace.

We define drip irrigation as an irrigation method in which, the water drips into the soil and slowly into the roots of plants. Due to this, it’s one of the most efficient methods because water is applied only there which is necessary preventing losses from evaporation. For the release of water droplets in each plant and the reduction of pressure, emitters are applied. They are divided into two categories: pressure compensating (PC) and non-compensating emitters (NPC). The difference between them is that PC emitters maintain the same flow rate for different inlet water pressures while NPC emitters giving different outputs for different inlet water pressures. NPC emitters are applied in lands without big slopes (hills, changes of terrain) or long rows so the pressure differences consider to be small. For difficult topographical conditions, PC emitters are used. Although, the current PC emitters require high pumping pressure in order to achieve flow stability, which means high cost in pumping machines and power systems, making them inefficient. Starling resistor is considered to be able to replace this kind of emitters.

Starling resistor is an experimental device which consists of a needle valve, a static pressure chamber and a collapsible elastic tube inside which is attached in two O-rings sealed caps, *Figure 1.5*.

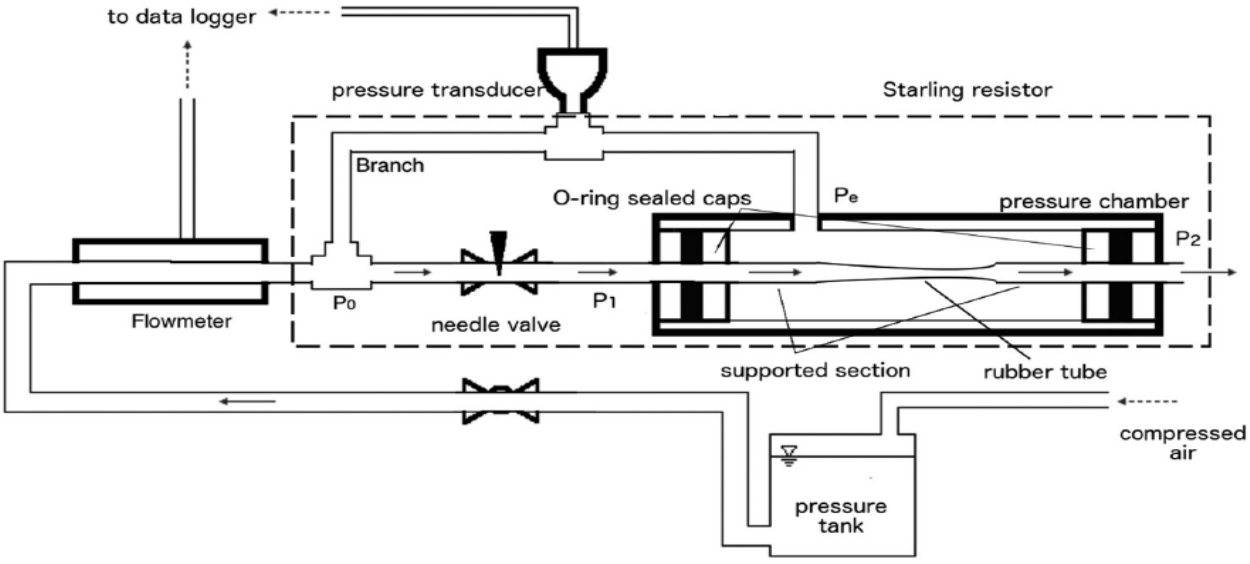

Figure 1.5: Experimental setup of Starling Resistor

The basic mechanism that takes place is called ‘’flow limitation’’ or ‘’pressure compensation’’ and is similar to the phenomenon which occurs in human lungs during forced expiration. According to this, after reaching a critical point of pressure (activation pressure) a further increase in driving pressure ($\Delta P = P_1 - P_2$: pressure difference between inlet and outlet of elastic tube) will not affect the flow rate.

To achieve this, the fluid, in our case water, has to pass from different parts inside the chamber. It starts flowing from pressure tank until it meets T-junction, as it is shown in *Figure 1.5*, in which it is divided into two different flows. The one part supplies the chamber, outside the tube, in order to exploit its static pressure (P_e). The second part passes a needle valve which decreases its lateral pressure from P_o or P_e to P_1 before entering the tube. In this way, the steady external pressure narrows the cross-section area as its value is greater than inlet pressure. As the fluid keeps flowing inside the elastic tube it loses further energy due to friction. This leads to further narrowing of the cross section area which will cause a rapid increase in flow resistance (Flow resistance $= 8\mu L / \pi \mathrm{R}^4$ [**Hagen-Poiseuille equation**]) and a conversion of lateral pressure to dynamic pressure. At some point the velocity of water is equal to the wave propagation speed. This condition is critical for achieving flow limitation *(E.A. Elliott, S.V. Dawson, 1977)* because if satisfied the tube narrows the most, flow limits and the flowrate gets the maximum value $\Phi_{\max}$ which cannot be exceeded. Increasing pressure difference after you reach these conditions will not cause an increase in flowrate. Comparing with current PC emitters, experimental measurements showed that Starling resistor is more efficient as it requires lower pumping power in order to keep flowrate constant *(Wang, Ruo-Qian, Teresa Lin, Pulkit Shamshery, Amos G. Winter,2016, http://hdl.handle.net/1721.1/109244).*

Except from the applications mentioned above which are artificial constructions, the phenomenon of fluid transportation inside a deformable path appears also in natural systems. The human body is one of these systems in which many elastic paths exist to ensure the transportation of necessary substances such as proteins, carbohydrates, vitamins, lipids and oxygen. For this purpose, responsible are arteries as they carry blood with oxygen (except pulmonary arteries which carry de-oxygenated blood) and nutrients from the heart to the entire body. When this procedure finishes, the opposite flow of blood begins and is accomplished with the contribution of less muscular elastic tubes called veins. Veins transport low-oxygenated and high-carbon dioxide blood (except pulmonary veins which carry oxygenated blood), from the human organs and tissues to the heart. Afterward, the heart pumps and forces blood to move inside the lungs to remove carbon dioxide.

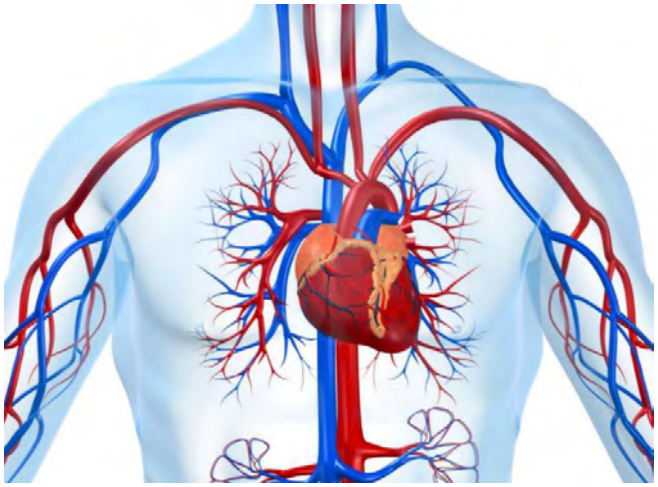

Figure 1.6: The network of arteries (red) and veins (blue) inside human body

Inside the lungs, we can find a network of thin elastic airways, in various sizes, called bronchioles which have an important role in breathing. During the process of inspiration, the air passes through the bronchioles' tree until it reaches an airway elastic sack called alveoli. When the air reaches alveoli a gas exchange procedure takes place between the capillaries and alveoli. Oxygen passes two thin layers of wall, first the wall of alveoli and then the capillary wall. After that, oxygen diffuses into the blood, inside the capillaries, and is transferred to the heart through pulmonary vein. Simultaneously with oxidation of blood, carbon dioxide, which is transported through the pulmonary arteries, passes the capillary wall and then the alveoli wall. In this way, diffuses into the air and it is removed from the human body through the air of expiration.

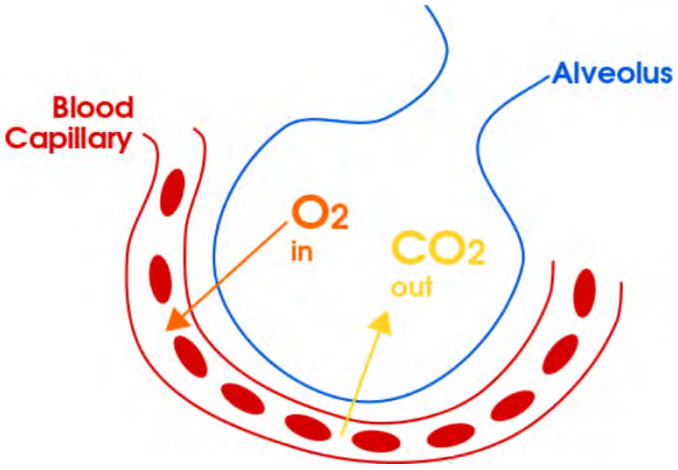

Figure 1.7: Gas exchange between alveoli and capillary

All these applications and many more, justify the need of a model that predicts the behavior of the flow through such systems. Our main goal is to examine a specific model for the flow of a fluid in a single deformable tube in different tension states. This is the basic component for many simulations that describe a variety of phenomena, some of which are mentioned in this chapter.

2. Material mechanics of rigid and flexible tubes

The equations that determine the state of a tube under tension are a key component of the problem this thesis examines. Thus, we need to build them starting from the basics. At first, we review some of the major concepts from material science, such as deformation and conservation laws, and then step by step apply them on a thin-shell cylindrical pipe to create a simplified model that describes the relationship between diameter of the cylinder and transmural pressure acting on it. Eventually, more complicated models will be presented, as well as an experimental one for the elastic compliance of lung airways proposed by *Lambert (1982)*. His model will be used for the computations in the following chapters.

2.1 Basics of material mechanics

In this paragraph we do a shallow dive in the vast field of material mechanics and introducing its fundamental concepts and equations. This is an attempt to figure out the complexity that is related to our problem, rather than try solving the material model that arises here.

Mechanics of material is the field of science that describes and predicts the behavior of solid objects under external load. For this purpose, the properties of material need to be considered too.

When a force acts on a solid structure, energy is added to the system and, due to conservation of energy, the state of material has to change. So, either a kinetic change or deformation (or both simultaneous) will occur, depending on the environmental conditions and the assumptions. We will analyze only the second effect independently, by assuming that the body is always fixed in place (static). In this case the entire external energy is transformed into deformation.

Deformation can be plastic (permanent change of shape) or elastic (reversible change). Almost every material deforms elastically at low loads and after a certain value of tension (yield stress σ_y) plastic deformation begins.

For this analysis, we are interested only in the first region of deformation, the elastic part of it. In science of materials, the most characteristic property that measures the elasticity is Young's modulus E. It is defined as $E = \frac{\sigma}{\varepsilon}$ which is the ratio of uniaxial stress σ over strain (proportional

deformation) ε and has units of pressure. A typical graph $\sigma-\varepsilon$ of a material, which results from tensile test, is presented next.

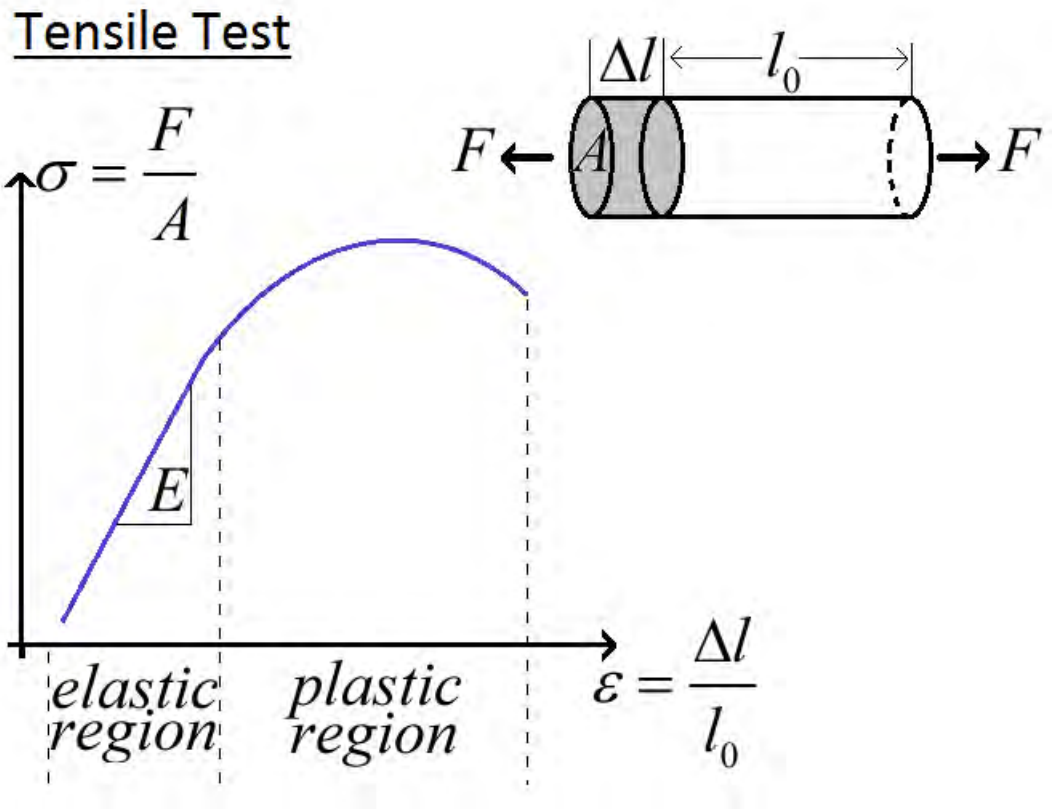

Figure 2.1.1:In tensile test a sample (of some material) with a cross-sectional area A is subjected to a continuously growing tension $\sigma = \frac{F}{A}$ and the consequential deformation $\varepsilon = \frac{\Delta l}{l_0}$ is measured.

Then, with this data we can plot the function of $\sigma(\varepsilon)$ in a diagram. This graph represents the behavior of this material under tension and as a consequence some of the basic properties of it can be determined.

Most solid industrial materials appear to have a constant E in the elastic region, which means the deformation changes linearly to the applied stress. However, there are materials, also, which have non-linear behavior. In very elastic materials (non-metallic, polymers, biomaterials, etc.) the elastic region is significantly bigger and thus the divergence from linearity is more common.

Another aspect of material mechanics, which has to be mentioned here, is that stress and strain are tensors. This means they consist of 9 components each, in general case. So at any point of the material we have to determine 9 values for each of those 2 quantities. Fortunately, some values of these tensors are negligible and can be ignored almost at any problem.

Boundary value problem

In order to continue with the solution of any problem in mechanics of material, we have to introduce first the fundamental equations and principles of this field. The basic equations that govern any material problem derive from 3 major principles and laws *(N. Aravas, 2014)*:

- **Newton's laws of motion (mechanical equilibrium):** Equations that derive from the balance between net and inertial forces acting on a body.
- **Constitutive model:** The relation between the applied load (stress σ) and the behavior of the object in terms of deformation ε that characterizes the material.
- **Compatibility of the medium:** Equations that describe the necessary and sufficient conditions under which a displacement field, that corresponds to a specific deformation input (strain ε), can exist.

These are the **field equations** of any problem that needs to be satisfied inside the material's body.

For example, the field equations that describe a **linear elastic material** in a compact form are:

- $\nabla \cdot \sigma + \rho b = 0,$ (3 equilibrium equations)
- $\sigma = \mathbf{L} : \varepsilon,$ (6 constitutive equations)
- $\varepsilon = \frac{1}{2}\left(u\tilde{\nabla} + \nabla u\right),$ (6 compatibility equations)

where u is the displacement vector, ε the infinitesimal strain tensor, σ the stress tensor, ρ the density of the material, b the vector of the body forces and $\mathbf{L}$ the elastic tensor of the material.

Finally, we have to add the material-environment interaction to completely define the problem. Boundary equations are necessary to fully describe the problem and have a strong impact on the solving method and the resulting solution of the problem.

The field equations coupled with the boundary conditions are called the **boundary value problem** and its solution determines the values of u, ε and σ at every point of the body.

2.2 Constitutive equations for a thin-shell cylinder

The problem we examine here, consists of a thin cylindrical tube (thickness<<length), a fluid inside with variable pressure along length axis and an external uniform pressure field acting on the outside shell of the tube.

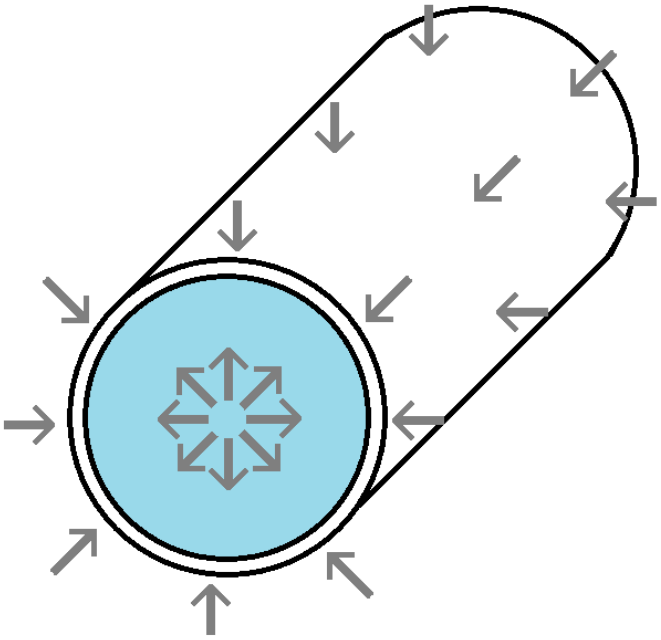

Figure 2.2.1: A thin cylindrical tube with external and internal load

According to the above paragraph 2.1, the set of equations with a linearly elastic approximation, that fully describes the static state of the tube, consists of 15 in total equations (9 partial differential and 6 algebraic) coupled with the boundary conditions. Such a problem requires a lot of parameters to be evaluated and the solution almost certainly will be computational (e.g. Finite Element Method). For the purposes of this study, such a model is not feasible so we will use a different approach. This approach exploits the cylindrical symmetry of the tube and the small thickness of its wall.

At first, we examine the forces acting on a small radial portion of the circular cross-section which is shown below in *Figure 2.2.2*:

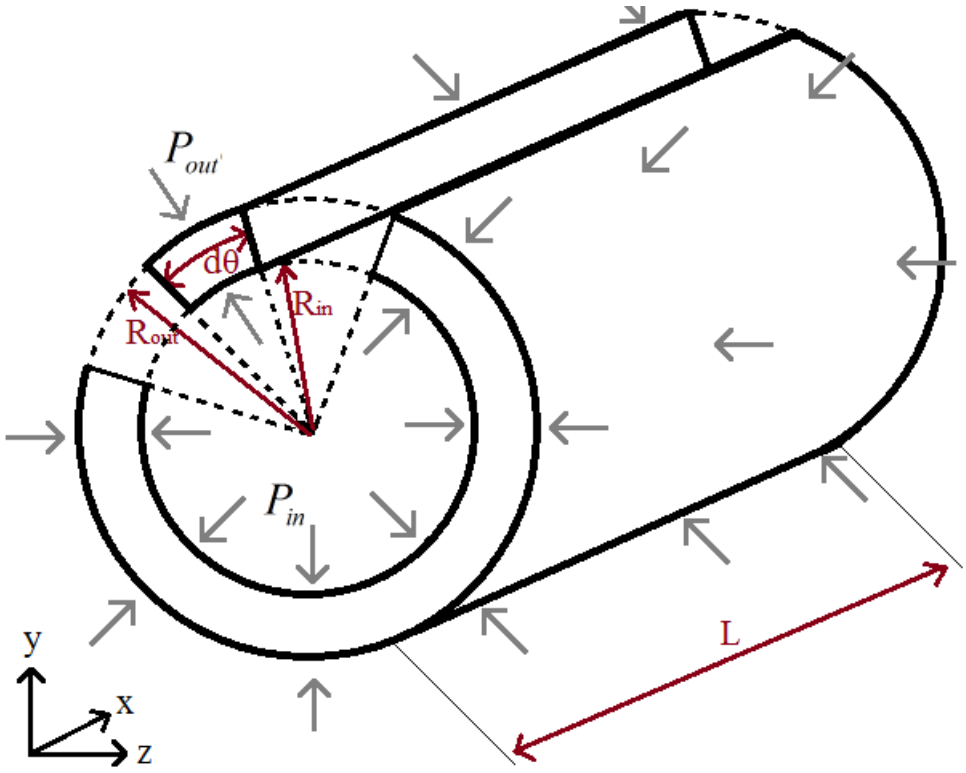

Figure 2.2.2: The direction of internal and external forces in a differential $d\theta$ portion of a thin cylindrical tube

The radial differential force dF_r acting on an infinitesimal $d\theta$ portion of the cylinder can be expressed as:

$$dF_r = dF_{in} - dF_{out} = P_{in}dA_{in} - P_{out}dA_{out} = P_{in}R_{in}Ld\theta - P_{out}R_{out}Ld\theta = \left(P_{in}R_{in} - P_{out}R_{out}\right)Ld\theta$$

$$\Rightarrow dF_r = \left(P_{in}R_{in} - P_{out}R_{out}\right)Ld\theta \qquad (1),$$

where $P_{in} = P_{in}(x)$ is the pressure of fluid at x, P_{out} the external pressure and R_{in}, R_{out}, L the geometrical characteristics of the tube (inside radius, outside radius, length).

Next we analyze the equilibrium of forces on the upper half-cylinder that derives from a section at x-z plane.

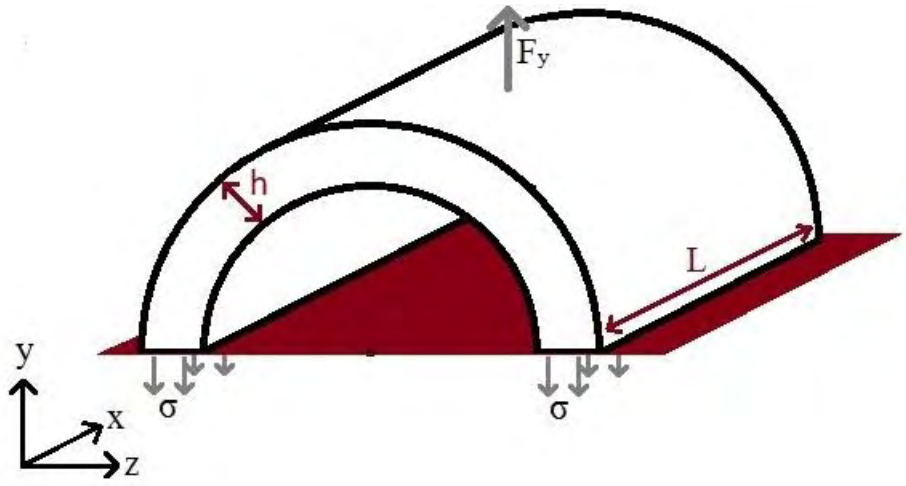

Figure 2.2.3: A cross sectional view of the upper half-cylinder with the acting forces

The vertical component of the force at y-axis, dF_y, can be calculated geometrically.

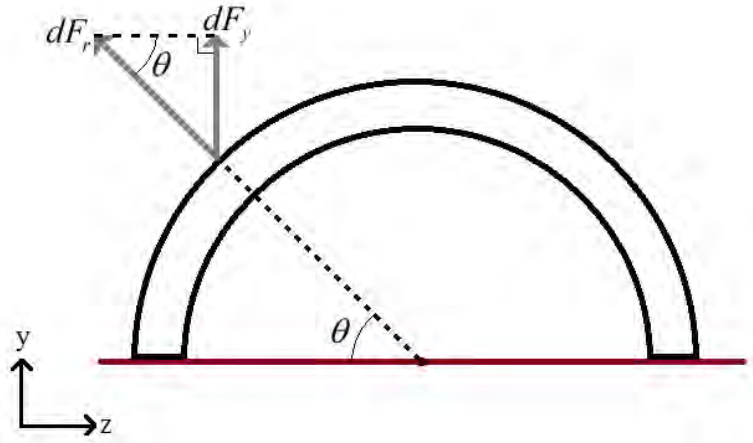

Figure 2.2.4: The vertical component dF_y of radial differential force dF_r.

$$\sin\theta = \frac{dF_y}{dF_r} \Rightarrow \quad dF_y = dF_r \sin\theta = \sin\theta\left(P_{in}R_{in} - P_{out}R_{out}\right)Ld\theta$$

After replacing, we can calculate the total vertical force F_y, acting on the upper shell, by integrating:

$$F_y = \int_0^{\pi} dF_y = \int_0^{\pi} \sin\theta\left(P_{in}R_{in} - P_{out}R_{out}\right)Ld\theta = \left[-\cos\theta\left(P_{in}R_{in} - P_{out}R_{out}\right)L\right]_0^{\pi} =$$
$$= \left(P_{in}R_{in} - P_{out}R_{out}\right)L - \left[-\left(P_{in}R_{in} - P_{out}R_{out}\right)L\right] \Rightarrow$$

$$\Rightarrow F_y = 2L\left(P_{in}R_{in} - P_{out}R_{out}\right) \qquad (2)$$

Since cylinder is stationary, mechanical equilibrium at y-axis can be written:

$$\Sigma F_y = 0 \Rightarrow\ F_y - F_\sigma = 0 \Rightarrow\ F_y - \sigma \cdot 2hL = 0$$

So, the net force acting on the half-cylinder (due to the difference in pressures) must be canceled out from the internal wall tension of the pipe.

To calculate this tension, we need to consider a constitutive model that will allow us to relate σ with the deformation ε, considering also the material properties. We will start by using the simplest model which is the linear one, also referred as Hooke's Law.

$$\sigma = \mathrm{E} \cdot \varepsilon \quad , \varepsilon = \frac{1}{\left(1-\nu^2\right)} \frac{R - R_0}{R_0}$$

Now we are ready to combine all the above and result in an equation that correlates diameter D with pressure $P_{tm}\left(= P_{in} - P_{out}\right)$.

$$F_y - \sigma \cdot 2hL = 0 \ \Rightarrow\ \ 2LR\left(P_{in} - P_{out}\right) = \sigma \cdot 2Lh \Rightarrow\ \ P_{tm} R = \varepsilon \cdot \mathrm{E} \cdot h$$

$$\Rightarrow\ \ P_{tm} R = \frac{1}{\left(1-\nu^2\right)} \frac{R - R_0}{R_0} \cdot \mathrm{E} \cdot h \ \Rightarrow\ \ P_{tm} = \frac{1}{\left(1-\nu^2\right) R} \frac{R - R_0}{R_0} \cdot \mathrm{E} \cdot h \Rightarrow P_{tm} = \frac{\mathrm{E} \cdot h}{\left(1-\nu^2\right) R} \left(\frac{R}{R_0} - 1 \right) \quad (3)$$

$$\Rightarrow\ P_{tm}(D) = \frac{2 \cdot \mathrm{E} \cdot h}{\left(1-\nu^2\right) D} \cdot \left(\frac{D}{D_0} - 1 \right) \ \ or \ \ D\left(P_{tm}\right) = \frac{2EhD_0}{2Eh - P_{tm}\left(1-\nu^2\right) D_0}$$

2.3 Analytical tube models

The Equation (3), which was obtained as a result of Hooke's Law, is the general form which corresponds in every tube with elastic behavior. By applying some extra assumptions, it is possible to derive new relations between pressure and diameter as shown in *table 1*:

Author	$p - A$ Relation
Rammos *et al.* (1998) [11]	$A = A_0\left[1 + \frac{D_0}{E\,h}(p - p_{ext})\right]$
Olufsen *et al.* (1999) [12]	$p - p_{ext} = \frac{4}{3}\frac{E\,h}{R_0}\left(1 - \sqrt{\frac{A_0}{A}}\right)$
Sherwin *et al.* (2003) [14]	$p = p_{ext} + \frac{\sqrt{\pi}\,E\,h_0}{(1-v^2)\,A_0}(\sqrt{A} - \sqrt{A_0})$
Urquiza *et al.* (2006) [15]	$p = p_{ext} + \frac{E\,h_0}{R_0}\left(\sqrt{\frac{A}{A_0}} - 1\right)$

*Table 1: Linear and non-linear Pressure-Area relations (*https://hal.archives-ouvertes.fr/hal-01807385/document)

Considering that Poisson's ratio is equal to zero $v = 0$ (materials such as cork) and assuming , also, $\frac{R}{R_0} = \frac{A}{A_0}$ which is acceptable only for small deformations the equation (3) will become similar to Rammos equation in table 1. In Olufsen equation a more accurate and valid relation between radius and surface is obtained $\frac{R}{R_0} = \frac{\sqrt{A}}{\sqrt{A_0}}$ while Poisson's ratio gets maximum value $v = 0.5$ (perfect incompressible isotropic material as Rubber). The last two equations have an important difference from the previous ones. They include an extra assumption about the variation of wall thickness. In these relations, the wall thickness was considered to remain constant h_0 and equal to the value $h_0 = \frac{h * R}{R_0}$ which is derived from an area conservation equilibrium $2\pi Rh = 2\pi R_0 h_0$. In first relations the wall thickness change for every different value of P_{tm}. Furthermore, observing more carefully the Sherwin and Urquiza equations we will see that Urquiza's relation is a specific case of general Sherwin's form and emanates from the fact that the value of Poisson's ratio was replaced with zero $v = 0$.

2.4 Lambert's experimental model for lung airways

The above analysis constitutes a general overview of the behavior of deformable tubes. Specifying and deepening this analysis to the objectives and targets of this thesis, we are focusing on the behavior of elastic tubes inside the human lungs. Thus, we consider more extensively the lung's structure and the model that corresponds to this.

As mentioned also in introduction, each human lung consists of many short in length and small in diameter elastic paths (bronchioles) which are responsible to transport the air from the outside environment and mouth to the air sacs (alveoli). To understand this better, it's necessary to illustrate these components and the general anatomy of the lung. In this thesis, we present the simplest structural model which was developed by Lambert et al. *(Lambert, Wilson, Hyatt, Rodarte, 1982)* and relies on Weibel's tracheobronchial tree model *(Weibel, 1963)* as shown in Figure 2.4.1.

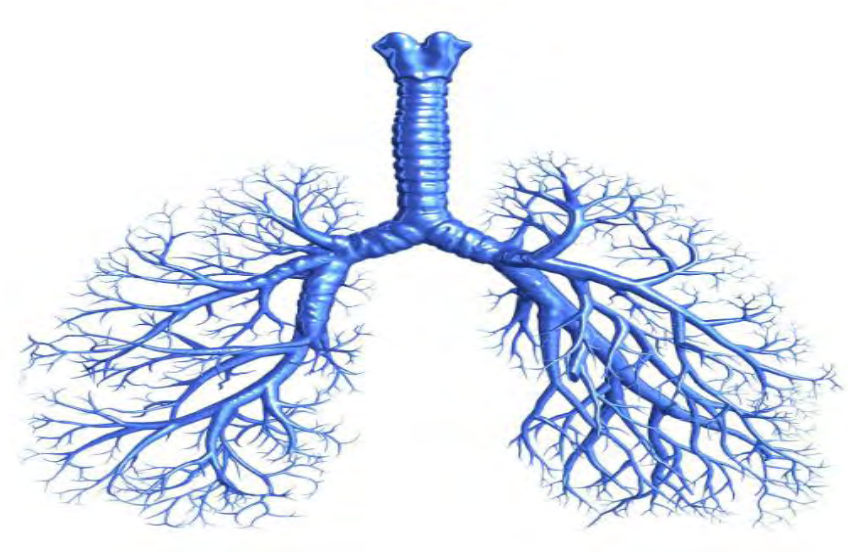

Figure 2.4.1: Weibel's Tracheobronchial tree model

Due to the complexity of lung structure, Lambert's model separates the bronchioles into classes according to common mechanical properties. More specifically, are classified into 17 different generations starting from the trachea (generation z=0) and ending up in bronchioles that are leading to alveoli (generation z=16).

In previous analysis the relations that have been extracted were analyticals functions. In this case the equations between $D - P_{tm}$ are obtained by experimental process. The parametres and the mechanical

properties which are necessary to apply in equations are received ,also, from measurements made on them. The results are presented in the *table 2* below :

z	a_0	a'_0	n_1	n_2	Am, cm^2	L, cm
0	0.882	0.000011	0.50	10.00	2.37	12.00
1	0.882	0.000011	0.50	10.00	2.37	4.76
2	0.686	0.000051	0.60	10.00	2.80	1.90
3	0.546	0.000080	0.60	10.00	3.50	0.76
4	0.450	0.000100	0.70	10.00	4.50	1.27
5	0.370	0.000125	0.80	10.00	5.30	1.07
6	0.310	0.000142	0.90	10.00	6.50	0.90
7	0.255	0.000159	1.00	10.00	8.00	0.76
8	0.213	0.000174	1.00	10.00	10.20	0.64
9	0.184	0.000184	1.00	10.00	12.70	0.54
10	0.153	0.000194	1.00	10.00	15.94	0.47
11	0.125	0.000206	1.00	9.00	20.70	0.39
12	0.100	0.000218	1.00	8.00	28.80	0.33
13	0.075	0.000226	1.00	8.00	44.50	0.27
14	0.057	0.000233	1.00	8.00	69.40	0.23
15	0.045	0.000239	1.00	7.00	113.00	0.20
16	0.039	0.000243	1.00	7.00	180.00	0.17

Table 2: Lambert's parameters of bronchial mechanical properties

The second column $a_0 = \frac{A_0}{A_m}$ expresses the ratio of surface $A = \frac{\pi * D^2}{4}$ at point $P_{tm} = 0$ to the maximal surface of current bronchiole $A_{m,1bronc} = \frac{A_m}{N_{total}} = \frac{\pi * D^2_{\max}}{4}$ in a specific generation ($N_{total} = 2^z$, z : number of generation) while the derivative of this ratio at the same point is demonstrated by the variable $a_0' = \left.\frac{da}{dP_{tm}}\right|_{P_{tm}=0}$ .The variables n_1, n_2 are exponential parameters and L is the length of bronchiole.

The branch experimental function which relates the pressure and diameter is expressed by two rectangular hyperbolae matching at point $P_{tm} = 0$:

- $D(P_{tm}) = D_{\max}\sqrt{a_0(1-\frac{P_{tm}}{P_1})^{-n_1}}$ if $P_{tm} < 0$
- $D(P_{tm}) = D_{\max}\sqrt{1-(1-a_0)(1-\frac{P_{tm}}{P_2})^{-n2}}$ if $P_{tm} \geq 0$

where $P_1 = a_0 n_1 / a'_0$ and $P_2 = -n_2(1-a_0)/a'_0$

These state laws of Lambert can be applied in every generation ,*Figure 2.4.2.* , to predict the diameter $D(P_{tm})$ for a fixed value of pressure $P_{tm} = P_{in} - P_{pleural}$ or the inverse.

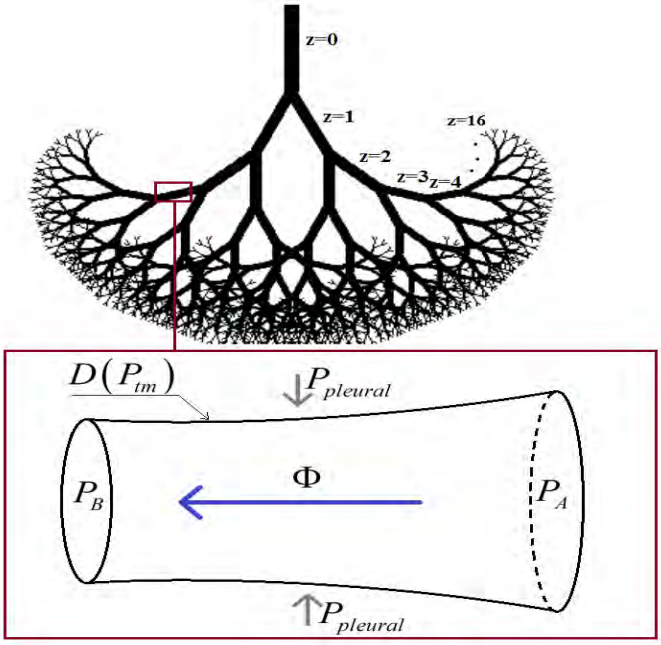

Figure 2.4.2: A demonstration of the basic's variables in a single bronchiole

To have a more clear view of the way that the ratio $a = \frac{A}{A_{m,1bronc}} = \frac{D^2}{D_{\max}{}^2}$ and derivative $a' = \frac{da}{dP_{tm}}$ variates , we have produced the following graphs ,using *Excel* ,for different values of P_{tm} . The range of transmural pressure that considered was from $-12\ cmH_20$ to $23\ cmH_20$.

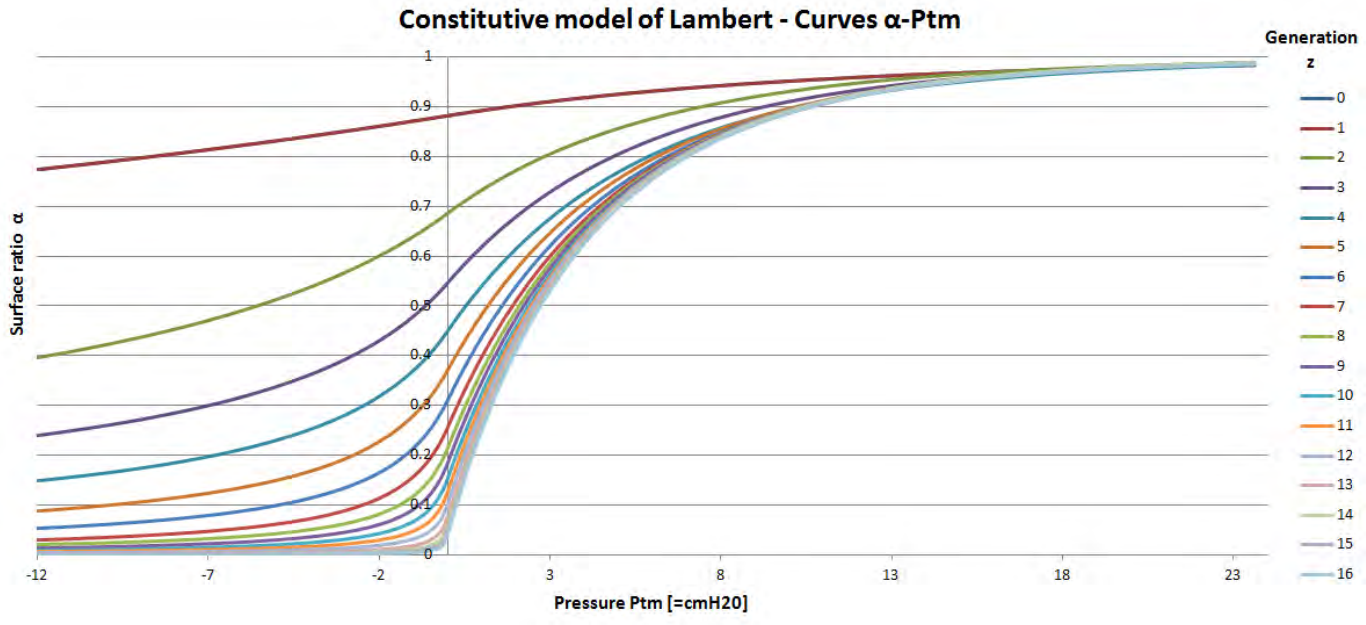

Figure 2.4.3: The variation of surface ratio (a) as transmural pressure (P_{tm}) changes for each generation ($z = 0-16$)

The intersection points between the curves and the y-axis, where $P_{tm} = 0$, are given by table 1. Before and after this point we can notice the 2 different curvature hyperbolae. For a range of transmural pressure between -7 cmH_20 and 8 cmH_20, all curves present larger slopes which means greater variations in surface area. So, we can infer that the change in diameter within this range of pressure will be greater than which would occur at values outside this range.

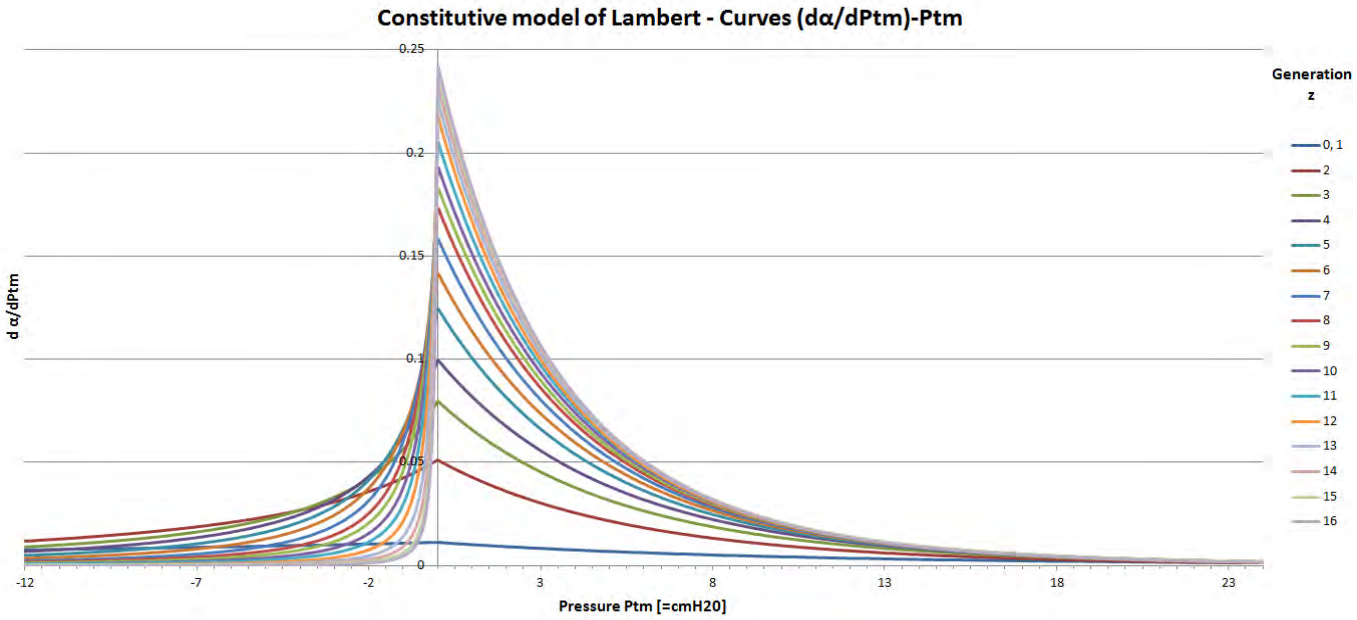

Figure 2.4.4: The relation between the derivative of surface ratio ($a' = \frac{da}{dP_{tm}}$) and transmural pressure (P_{tm}) for each generation ($z = 0-16$)

The above curves have absolute maximum at $P_{tm} = 0$ which means that the slope of $a - P_{tm}$ curves will become maximum at this point for every generation. According to this and comparing the values of derivative at $P_{tm} = 0$, we understand that the bronchioles become more flexible at higher generations, i.e. deeper in the lung.

3. Airflow in a single bronchiole

Case study: Airflow in a single airway

In this chapter we develop the equations which model the flow of air through an elastic tube. We examined the constitutive equation of the pipe in terms of $D(P_{tm})$ from previous chapter and now are ready to build a model for the inner flow of air using principles from fluid mechanics. The key assumption of the analysis that follows is that of steady state. This means that all parameters of the problem (i.e. tube diameter, air flow rate etc) remain temporally constant, though they may vary spacially, and in particular in the axial direction.

Conservation laws are axioms that derive from observations in nature. They are used as fundamental tools of science to build more complicated laws that predict the behavior of other natural systems. Conservation of energy and mass are two examples of axioms since they cannot be proved but they accurately describe everything we have observed around us until today. Starting from those two basic principles we present a model for airflow in an airway.

3.1 Bernoulli's principle

3.1.1 Mass and energy equilibrium

In open systems, where mass is flowing in and out from the boundaries of the system, the conservation laws of mass and energy can be expressed as the following equilibriums.

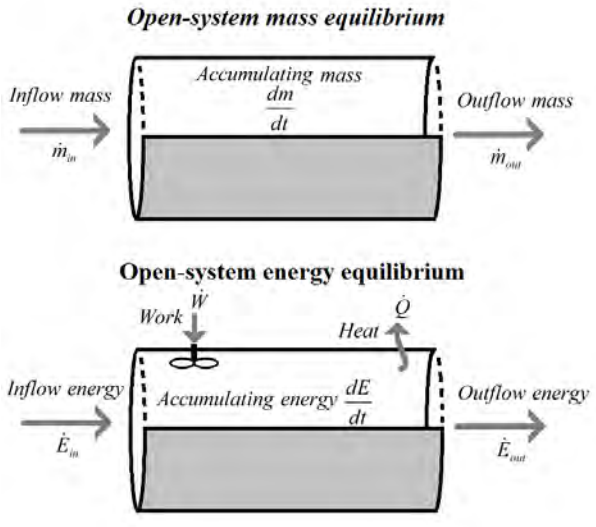

Figure 3.1.1: Mass and Energy equilibrium in an open system

Total mass equilibrium [kg/s]:

$$Accumulating\ mass\ =\ Inflow\ mass\ -\ Outflow\ mass$$

or in mathematical terms:

$$\frac{dm}{dt} = \dot{m}_{out} - \dot{m}_{in} = \Phi_{out}\rho - \Phi_{in}\rho$$

Assumptions:

- $steady\ state: \frac{dm}{dt} = 0$

Next, we apply the assumptions to get:

$$\left.\begin{array}{l} \frac{dm}{dt} = 0 \Rightarrow \Phi_{out}\rho_{out} - \Phi_{in}\rho_{in} = 0, \\ Incompressible\ \ flow: \rho_{out} = \rho_{in} = \rho \end{array}\right\} \Rightarrow \Phi_{out} = \Phi_{in} = const = \Phi \qquad (1)$$

The resulting relation (1) confirms the intuition that the mass entering the system is equal to the outflow mass, since there is no accumulation and mass can neither be created or vanished.

Total energy equilibrium [J/s]:

$$Accumulating\ energy\ =\ Inflow\ energy\ -\ Outflow\ energy\ +\ Work\ -\ Heat$$

or in mathematical terms:

$$\frac{dE}{dt} = \dot{E}_{in} - \dot{E}_{out} + \dot{Q} - \dot{W}$$
$$\Rightarrow \frac{dE}{dt} = \Phi_0\left(P + \frac{1}{2}\rho u^2 + \rho g z\right)_0 - \Phi_x\left(P + \frac{1}{2}\rho u^2 + \rho g z\right)_x + \dot{Q} - \dot{W}$$

Assumptions:

- $\dot{W} = 0$
- $\dot{Q} = -\int_0^x \Phi(s)\, f(s)\, ds \left[= \frac{m^3}{s}\frac{Pa}{m}m = Watt\right]$, *where* $f(x)$ *is the friction losses per unit distance* $[= Pa/m]$

- $1D:\ \vec{u} = u(x)\,\mathrm{e}_x$
- *Solve for steady state* $\frac{d}{dt}E_{tot} = 0$
- *Incompressible flow*
- ρgz *negligible*

Applying these assumptions in the energy equations to get:

$$\Phi_0\left(P+\frac{1}{2}\rho u^2\right)_0 - \Phi_x\left(P+\frac{1}{2}\rho u^2\right)_x - \int_0^x \Phi(s)\,f(s)\,ds = 0 \qquad (2)$$

Finally, we combine the equations (1) and (2):

$$(2) \overset{(1)}{\Rightarrow} \Phi\left(P+\frac{1}{2}\rho u^2\right)_0 - \Phi\left(P+\frac{1}{2}\rho u^2\right)_x - \Phi\int_0^x f(s)\,ds = 0$$

$$\Rightarrow P_0 + \frac{1}{2}\rho u_0{}^2 - P(x) - \frac{1}{2}\rho u(x)^2 - \int_0^x f(s)\,ds = 0 \qquad (3)$$

3.1.2 The term f(x)

It is important to choose carefully the function f(x). Previous researches [*Lambert*] suggest the model of *Reynolds (1982)* derived from experimental data:

$$f(x) = \frac{128\eta\Phi}{\pi D^4(x)}\left(a + b\,\mathrm{Re}(x)\right) - \cancel{\rho g \cos\theta}$$

$$\Rightarrow f(x) = \frac{128\eta\Phi}{\pi D^4(x)}\left(a + b\,\mathrm{Re}(x)\right)$$

The first term in the equation above refers to viscous pressure loses for a Poiseuille flow. The scaling factor a accounts for increased friction due to the short airway (deviation from fully developed flow/unsteady conditions). For an infinite straight pipe a should be 1 as the velocity profile will have enough time to be developed. The second term refers to turbulent pressure dissipation which occurs in higher velocities. Based on Reynolds, *(Reynolds,1982)* these factors in the case of human lungs are $a = 1.5$ and $b = 0.0035$.

Equation (3) is Bernoulli's equation, augmented with the term which represent friction losses. We could stop and solve here, although because f(x) depends on D and we lack the information about the profile of D versus x, it is preferable to differentiate (3) in respect to x and try to solve the differential that arises. This procedure follows the analysis of *Filoche* and *Florens (2011)*.

3.2 The differential equation of pressure gradient

To avoid misunderstandings in calculations we considered: $P = P(x),\ D = D\left(P(x)\right),\ u = u\left(P(x)\right)$

We start by differentiate eq. (3) along x-direction:

$$\frac{d}{dx}\left(P_0 + \frac{1}{2}\rho u_0{}^2 - P - \frac{1}{2}\rho u^2 - \int_0^x f(s)\,ds\right) = 0$$

$$\Rightarrow -\frac{d}{dx}[P] - \frac{1}{2}\rho\frac{d}{dx}\left[u^2\right] - f(x) = 0$$

$$\Rightarrow \frac{dP}{dx} + 2\frac{1}{2}\rho u\frac{d}{dx}[u] + f(x) = 0 \quad (4) \qquad , where\ u(x) = \frac{\Phi}{A} = \frac{4\Phi}{\pi D(x)^2}$$

The derivative of u can be calculated next:

- $$\frac{d}{dx}[u] = \frac{d}{dx}\left[\frac{4\Phi}{\pi D^2}\right] = \frac{d}{dP}\frac{dP}{dx}\left[\frac{4\Phi}{\pi D^2}\right] = \frac{4\Phi}{\pi}\frac{dP}{dx}\frac{d}{dP}\left[\frac{1}{D^2}\right] = \frac{4\Phi}{\pi}\frac{dP}{dx}\left[\frac{-2}{D^3}\frac{dD}{dP}\right] =$$

$$= \frac{4\Phi}{\pi}\frac{1}{D^2}\frac{dP}{dx}\frac{-2}{D}\frac{dD}{dP} = -2u\frac{1}{D}\frac{dP}{dx}\frac{dD}{dP} \Rightarrow \frac{d}{dx}[u] = -2u\frac{1}{D}\frac{dP}{dx}\frac{dD}{dP}$$

Then we can replace the derivative in (4):

$$\frac{dP}{dx} = -\rho u\left[-2u\frac{1}{D}\frac{dP}{dx}\frac{dD}{dP}\right] - f(x) = 2\rho u^2\frac{1}{D}\frac{dP}{dx}\frac{dD}{dP} - f(x)$$

$$\Rightarrow \frac{dP}{dx}\left[1 - 2\rho u^2\frac{1}{D}\frac{dD}{dP}\right] = -f(x)$$

$$\Rightarrow \frac{dP}{dx} = \frac{-f(x)}{1 - 2\rho u^2\frac{1}{D}} = \frac{-f(x)}{1 - 2\rho u^2\frac{1}{D}\frac{dD}{dP}} = \frac{-f(x)}{1 - \frac{u^2}{c^2}}$$

Eventually, we get the following differential equation derived from Bernoulli equation (3):

$$\frac{dP}{dx} = \frac{-f(x)}{1-\frac{u^2}{c^2}} \qquad (5)$$

where $\frac{1}{c^2} = \frac{2\rho}{D}\frac{dD}{dP}$ $\left[= \frac{kg}{m^3}\frac{1}{m}\frac{m}{Pa} = \left(\frac{s}{m}\right)^2 \Rightarrow c = \frac{m}{s} \right]$, $c = \sqrt{\frac{D}{2\rho}\frac{1}{(dD/dP)}}$

The equation (5) is an expression of the gradient of pressure across the tube.

A closer observation at (5) can give us insights of this phenomenon and a better understanding of some interesting natural limits that arise.

3.2.1 The wave propagation speed c

Firstly, we have to give some meaning into the parameter c. It has units of velocity $\left[\frac{m}{s}\right]$ and depends on the tube's geometry and properties. Therefore, c is a characteristic velocity referred to the tube. More specifically, c is a function of density ρ, diameter D and $\frac{dD}{dP}$ derivative. The $\frac{dD}{dP}$ term contains information about the change in diameter as a result of pressure change and we can derive that depends on the elasticity of the wall. So, we can infer that the wave propagation speed expresses the speed of pressure disturbance along the tube.

3.3 The final algebraic equation

The analytical or numerical way of solving the differential equation can be avoided by transforming it to algebraic equation with some clever manipulations proposed by *Filloche* and *Florence (2011)*. To solve this equation for calculating the flow of air Φ, which is constant at any point throughout the tube, we can integrate (5) from A to B (full length of the tube), where P_A, P_B are given values.

$$\frac{dP}{dx} = \frac{-f(x)}{1-\frac{u^2}{c^2}} \Rightarrow D^4\left(1-\frac{u^2}{c^2}\right)\frac{dP}{dx} = -D^4 f(x)$$

$$\Rightarrow \int_A^B D^4\left(1-\frac{u^2}{c^2}\right)\frac{dP}{dx}dx = \int_A^B -D^4 f(x)dx \qquad (6)$$

- $\int_A^B D^4\left(1-\frac{u^2}{c^2}\right)\frac{dP}{dx}dx=\int_A^B D^4\left(1-\frac{u^2}{c^2}\right)dP=\int_A^B D^4\left(1-2\rho\frac{1}{D}u^2\frac{dD}{dP}\right)dP=$

$=\int_A^B D^4dP-\int_A^B 2\rho D^4\frac{1}{D}\left(\frac{4\Phi}{\pi D^2}\right)^2\frac{dD}{dP}dP=h(P_B)-\mathrm{h}\left(P_A\right)-\int_A^B 2\rho\frac{16\Phi^2}{\pi^2 D}dD=$

$=\Delta h_{\mathrm{A}}^{\mathrm{B}}-\frac{32\rho\Phi^2}{\pi^2}\left[\ln\left(D\right)\right]_{D_A}^{D_B}=\Delta h_{\mathrm{A}}^{\mathrm{B}}-\frac{32\rho\Phi^2}{\pi^2}\ln\left(\frac{D_B}{D_A}\right)$

- $\int_A^B -D^4(x)\,f(x)dx=\int_A^B -D^4\left(x\right)\frac{128\eta\Phi}{\pi D^4\left(x\right)}\left(a+b\,\mathrm{Re}\left(x\right)\right)dx=-\frac{128\eta\Phi}{\pi}\int_A^B\left(a+b\,\mathrm{Re}\left(x\right)\right)dx$

$=-\frac{128\eta\Phi}{\pi}\left(\int_{A:x=0}^{B:x=L} a\,dx+\int_A^B b\,\mathrm{Re}\left(x\right)dx\right)=-\frac{128\eta\Phi}{\pi}\left(aL+b\int_A^B \mathrm{Re}\left(x\right)dx\right)$

We can rewrite the equation (6) as,

$$\Delta h_{\mathrm{A}}^{\mathrm{B}}-\frac{32\rho\Phi^2}{\pi^2}\ln\left(\frac{D_B}{D_A}\right)=-\frac{128\eta\Phi L}{\pi}\left[a+b\left\langle\mathrm{Re}\right\rangle\right]\qquad(7)$$

with $\left\langle\mathrm{Re}\right\rangle=\mathrm{Re}_{average}=\frac{\int_A^B \mathrm{Re}\left(x\right)dx}{L}=\frac{1}{L}\int_A^B\frac{4\rho\Phi}{\eta\pi D(x)}dx=\frac{4\rho\Phi}{\eta\pi L}\int_A^B\frac{1}{D(x)}dx=\frac{4\rho\Phi}{\eta\pi\left(\frac{D_A+D_B}{2}\right)}\Rightarrow\left\langle\mathrm{Re}\right\rangle=\frac{4\rho\Phi}{\eta\pi\left(\frac{D_A+D_B}{2}\right)}$

4. Computations in a single airway

This chapter consists of our computations and efforts that we carry out to analyze how accurately that model simulates the flow of air inside one human lung airway. At first, we introduce the parameters and a modified version of the equation (7) that we are going to solve. A first sample of solutions is derived and then a systematic parametric analysis follows. Next we calculate the profile of pressure in a single tube by using two computational methods and we got some interesting results about the model of *Filoche* and *Florence*. The chapter continues with a suggestion of a different computational flow model and ends with a comparison between the two models that have been applied. In conclusion, the structure of the whole chapter follows the path we took chronologically to get into the details and the difficulties we faced as we deepen our understanding

4.1 Computation of flow rate

4.1.1 Computational process

We start from the written equation that has been mathematically proved in the previous chapter and after some arrangements at (7), we can get an expression for flow Φ.

$$(7) \Rightarrow h(\mathrm{P}_{tm,B}) - h(\mathrm{P}_{tm,\mathrm{A}}) - \frac{32\rho\Phi^2}{\pi^2}\ln\left(\frac{D_B}{D_A}\right) = -\frac{128\eta L\Phi}{\pi}\left[a + b\frac{4\rho\Phi}{\eta\pi\left(\frac{D_A+D_B}{2}\right)}\right]$$

$$\Rightarrow \Delta h_A^B = \frac{32\rho\Phi^2}{\pi^2}\ln\left(\frac{D_B}{D_A}\right) - \frac{128\eta L\Phi a}{\pi} - \frac{1024Lb\rho\Phi^2}{\pi^2\left(D_A+D_B\right)}$$

$$\Rightarrow \frac{1024Lb\rho - 32\rho\left(D_A+D_B\right)\ln\left(\frac{D_B}{D_A}\right)}{\pi^2\left(D_A+D_B\right)}\Phi^2 + \frac{128\eta La}{\pi}\Phi + \Delta h_A^B = 0$$

$$\Rightarrow k\Phi^2 + j\Phi + l = 0,$$

$$\text{where } k = \frac{1024Lb\rho - 32\rho\left(D_A+D_B\right)\ln\left(\frac{D_B}{D_A}\right)}{\pi^2\left(D_A+D_B\right)},\ j = \frac{128\eta La}{\pi},\ l = \Delta h_A^B$$

$$\Rightarrow \Phi = \frac{-j + \sqrt{j^2 - 4kl}}{2k} \quad (8)$$

This is an algebraic non-linear (quadratic polynomial) equation in respect to Φ. Given as inputs the pressures ($P_A, P_B, P_{pleural}$) of the system we can easily calculate the two solutions using the discriminant. Due to natural restrictions the negative solution is rejected and only the positive one is accepted (8). For this purpose a programming code in Fortran was written.

Since this flow is constant, as we already mentioned, we can calculate other variables at every point of the tube (such as velocity and diameter profiles) for this calculated Φ. Adding some extra subroutines on the previous code, we compute the diameter profile, the ratio of speeds u/c, local Reynolds number too.

4.1.2 Results

In the beginning, we start solving the equation (8) for a single airway tube with specific parameters $z, P_A, P_B, P_{pleural}$ to get the flow rate Φ through it. Some tests are presented in the *Table 3* below.

Test #	*Gen. z*	$L(z)[m]$	$P_A[Pa]$	$P_B[Pa]$	$P_{pleural}[Pa]$	$\Phi\left[\frac{l}{s}\right]$
1.	0	0.1200	1000	500	0	**5.026**
2.	0	0.1200	1000	200	0	**6.190**
3.	0	0.1200	1000	500	200	**4.928**
4.	0	0.1200	1000	500	1500	**4.108**
5.	3	0.0076	1000	500	0	**1.578**
6.	3	0.0076	1000	500	1500	**0.381**
7.	6	0.0090	1000	500	200	**0.196**
8.	9	0.0054	1000	500	0	**0.052**

Table 3: Values of flowrates Φ for a different couple of parameters $z, L, P_A, P_B, P_{pleural}$

Some primal results can be concluded here from *Table 1*, even if the sample of tests is very small.
A crucial notation that needs to be reminded is that every generation has a unique constitutive wall behavior. So, there is a hidden parameter that lies under the generation z value, which must be taken into consideration too.

- A greater $\Delta P = P_A - P_B$ increases the airflow Φ, since it is the driving force of the flow.
- A bigger $P_{pleural}$ strangles the pipe and reduces the Φ flow.

These results also agree with the intuition. However, as we will see in a more detailed examination next, they are not valid for every case.

Parametric analysis

To get a more precise picture, we solve the equation (8) parametrically for P_B and $P_{pleural}$ with the addition of an extra subroutine (Parametric_analysis) at the basic code. The results are condensed in one diagram that is presented next.

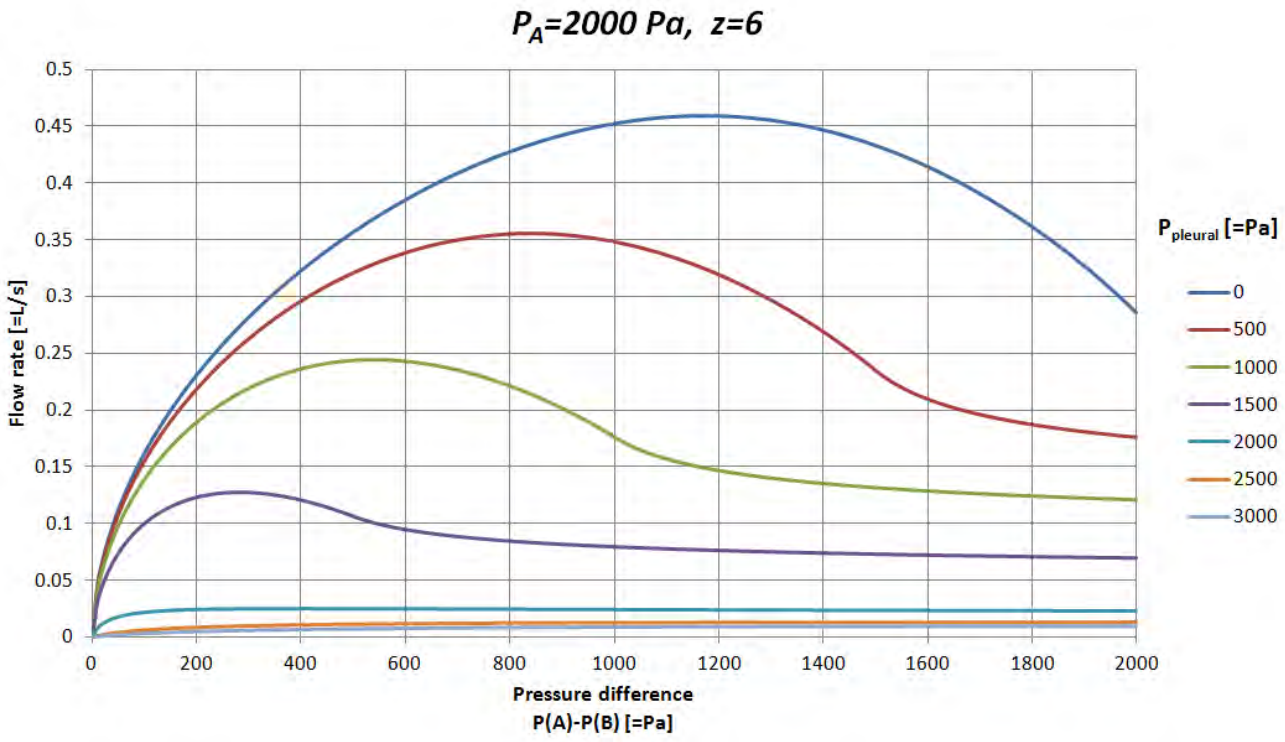

Figure 4.1.1: Φ - $\Delta P\left(P_A - P_B\right)$ *graph*

As the title of the graph suggests, these results refer to a pipe with constant parameters $P_A = 2000\,Pa$ and for generation $z = 6$. This is the general and representative picture of the diagrams we got for other P_A and z values too, which were only differentiated quantitatively. Thus, the analysis that follows below can be expanded and apply to other cases.

The values of P_B starts from 0 to and $P_{pleural}$ is given the discrete values $\{0, 500, 1000, 1500, 2000, 2500, 3000\}$. It is worth mentioning that although P_A remains constant, the transmural pressure $P_{tm,A}$ will change, since $P_{pleural}$ varies.

The first observation we can make immediately from the way that curves are stacking, is about the dependence of Φ in respect to $P_{pleural}$. Low $P_{pleural}$ curves are above the higher once for each $\Delta P(= P_A - P_B)$. We can confirm now that an increase in $P_{pleural}$ leads to a decrease in the airflow Φ.

A more interesting behavior appears when we examine the shape of the curves. First we can see that there are 2 types of curves. The curves for $P_{pleural}$ $\{0, 500, 1000, 1500\}$ that have a maximum value $\Phi_{\max}$ and the curves for $P_{pleural}$ $\{2000, 2500\}$ that increase at the start and then remain almost constant. More specifically, an example for each case will be examined next.

The curve for $P_{pleural} = 1000$ has a maximum at $\Delta P = 540\ Pa$ with a flow rate of $\Phi_{\max} = 0.244\ \mathrm{L}/s$ and after that point the airflow decreases and eventually at $\Delta P > 1400\ Pa$, Φ remains almost constant and independent of ΔP.

The curve for $P_{pleural} = 2000$ rises fast to a flow rate of $\Phi = 0.025\ \mathrm{L}/s$ and then remains constant around this value for the whole range of ΔP. This means that after a certain value of $P_{pleural}$ the airflow Φ is independent from the effort ΔP that we apply.

This is a very interesting and important result, which agrees with tests on human expiratory flow that was made (spirometry) and the same flow limiting phenomenon appeared.

An alternative view of the previous graph is the 3D diagram:

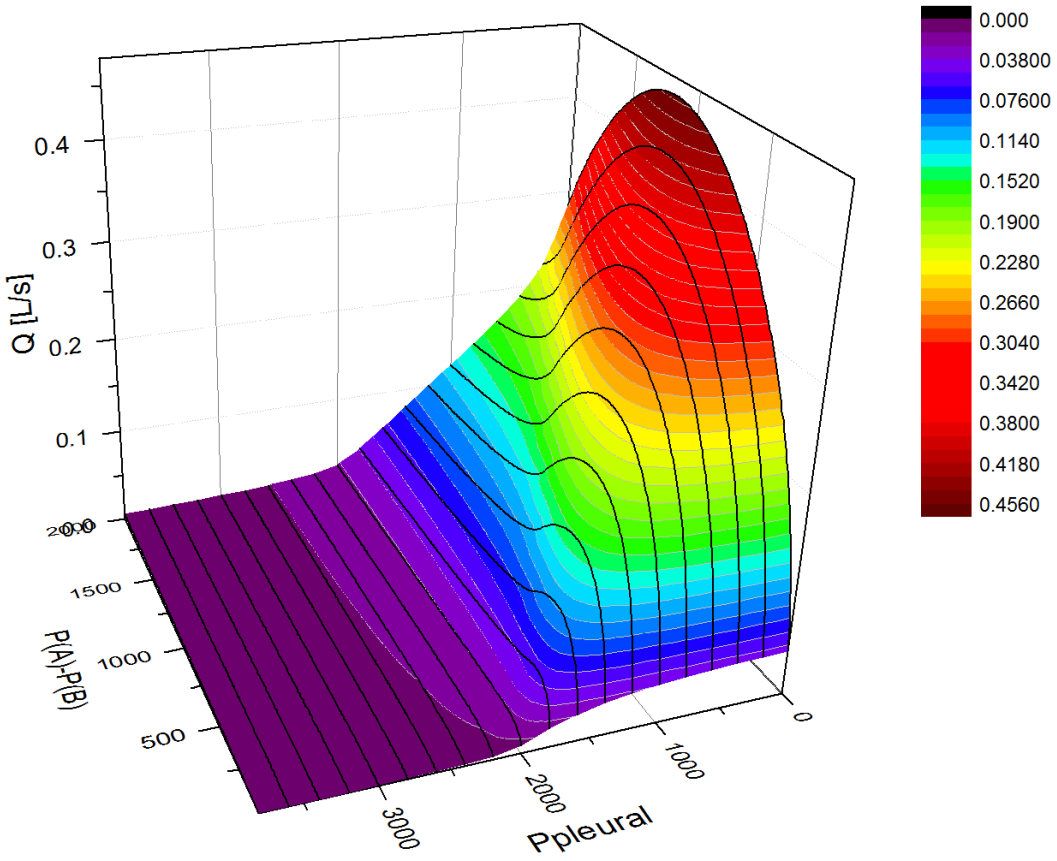

Figure 4.1.2: Parametric analysis in a 3-D graph

4.2 Calculation of Profile

A very intriguing question that arises next is what is happening along one of those tubes, especially those where flow limitation is observed. With that in mind, we try to calculate the profiles of $P(x)$, $u(x)$ and other parameters across $x-axis$ that will give us more insights of the flow limiting phenomenon.

The basic principle under which we create the algorithms for those profiles is the fact that flow rate Φ stays constant across the whole path of the pipe. (Although, we already explain in the construction of the model at Chapter III, that constant flow is an assumption and the flow of mass is 1D.)

4.2.1 First algorithm

At first, in order to compute the profiles we create the Profile_1 subroutine. This subroutine uses an iterative convergence method that guesses the outlet pressure P_x until Φ converges. The Figure contains a schematic diagram of the algorithm. In more detail, we start by calculate the flow Φ_0 through a pipe from equation (7) with parameters P_A, P_B, $P_{pleural}$, L. Then, we solve again the same equation but with parameters P_A, P_x^{est}, $P_{pleural}$, x. We discrete the L length into $N \cdot dx$ so that each space-iteration i has a length of $x = i \cdot dx$. For every x, by giving an initial estimation of outlet pressure P_x^{est} we calculate a new Φ_{est} and simply try to converge that Φ_{est} to the desirable Φ_0 by changing P_x^{est}. After convergence occurs $P_x = P_x^{est}$, $D_x = D(P_x)$ and $u_x = \dfrac{4\Phi_0}{\pi D_x^2}$ can be determined.

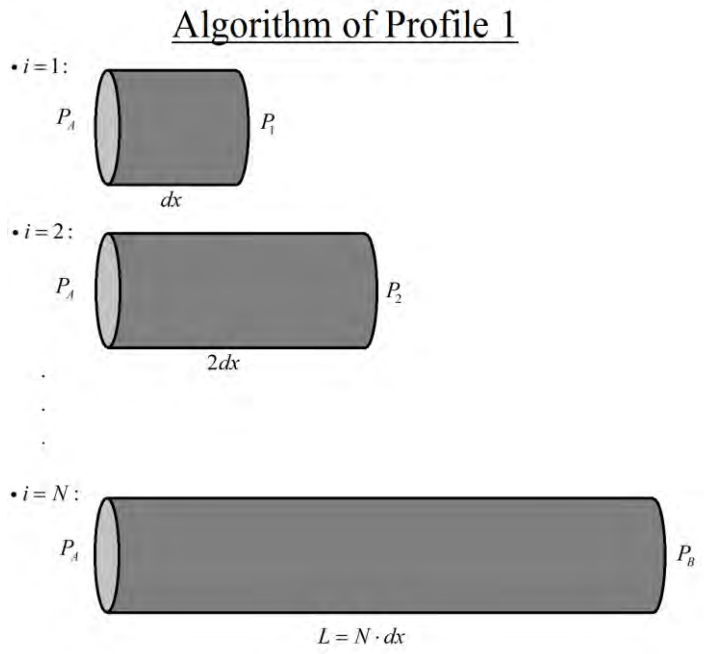

To sum up, this method functions as if it is computing the outlet pressures P_x of N tubes, each one of them has resulted from an internal iteration process until its Φ_{est} becomes the same as the flow Φ_0 (from the tube with length L).

Results of Profile_1

The curves that were calculated are realistic and acceptable for a sufficient range of values in which they were tested. In the following Figures, profiles of $P(x)$ and $D(x)$ are plotted.

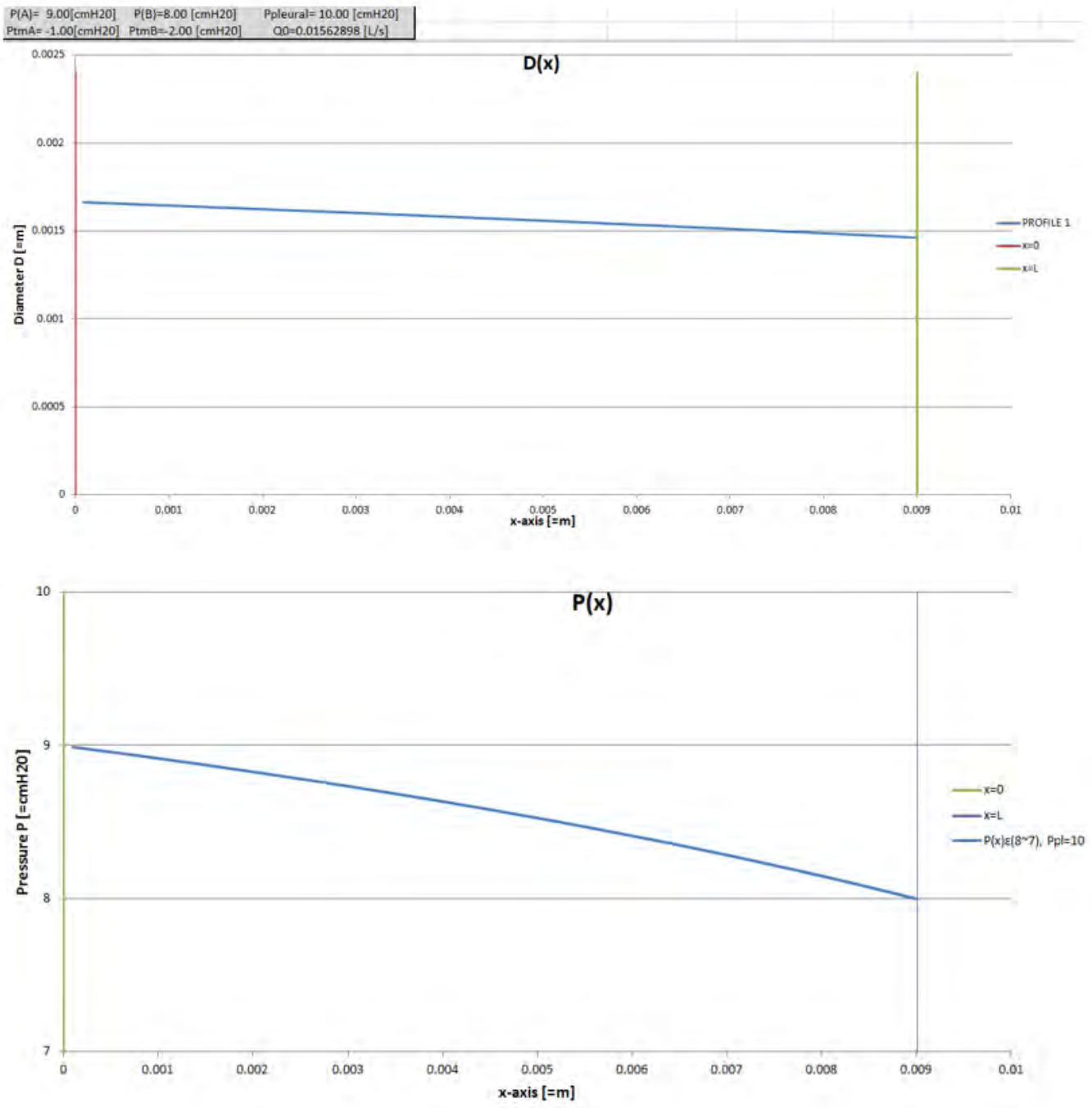

Figure 4.2.1 - 4.2.2: Profile of $D(x)$ *and* $P(x)$ *with a set of inputs* $\{P_A = 9\ cmH_2O\ ,\ P_B = 8\ cmH_2O\ ,$ $P_{pleural} = 10\ cmH_2O\ ,\ L = 0.009\ m\}$

On the other hand, there were cases of unnatural and infeasible solutions. An example is presented next.

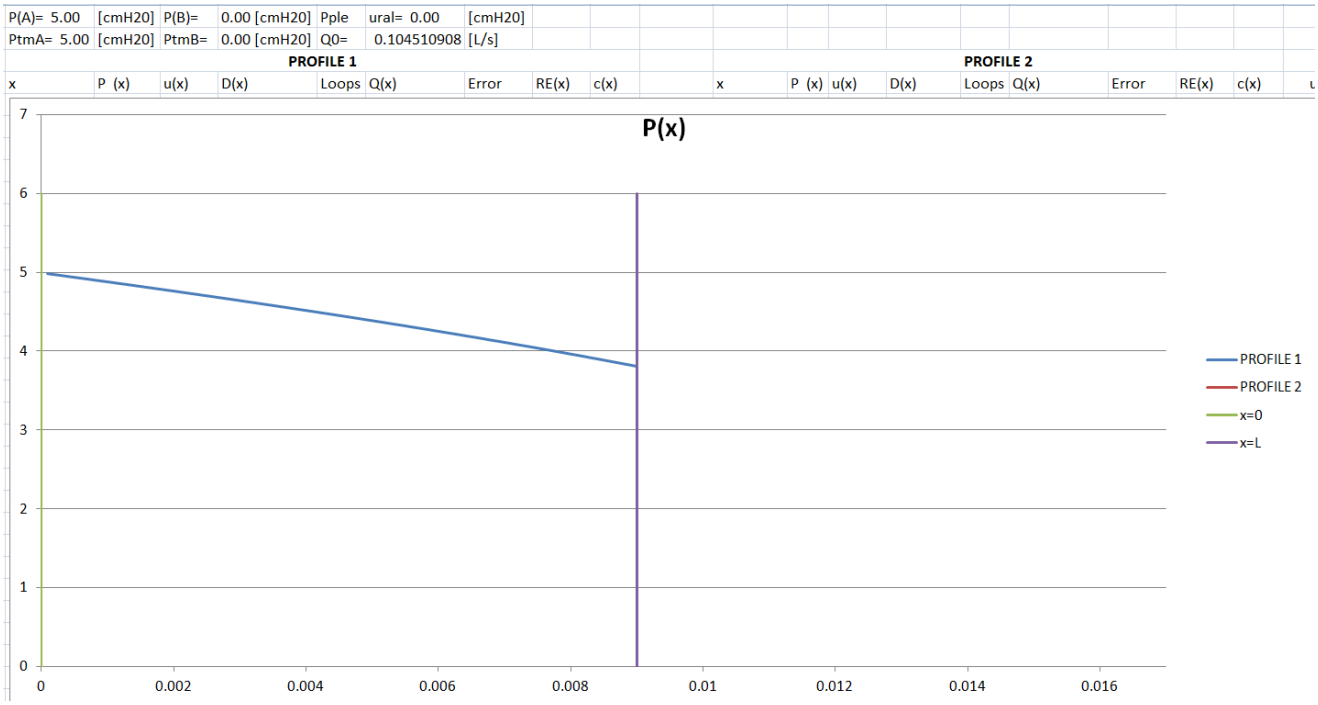

Figure 4.2.3: Problematic solution of Profile_1 of $P(x)$ *with a set of* $\{P_A = 5\, cmH_2O$,

$P_B = 0\, cmH_2O$, $P_{pleural} = 0\, cmH_2O$, $L = 0.009\, m\}$

The problem may not be clear at first here, but with a closer look we can see that the pressure at $x = L = 0.009\, m$ differs from the pressure we give as an input. Initially we calculate the flow $Q = 0.105\, L/s$ for a $\Delta P = P_A - P_B = 5 - 0$, and then the profile results with a total $\Delta P = P_A - P_B = 5 - 3.8$ only.

This was not a unique case, but under some circumstances this problem continues to appear. For this reason, we resort to another approach of the profile's calculation.

4.2.2 Second algorithm

In this case, instead of using the algebraic equation (7) we start from its differential form (5) which is:

$$\frac{dP}{dx} = \frac{-f}{1 - \frac{u^2}{c^2}} \qquad (5)$$

The idea behind this approach lies in the definition of the local derivative $\frac{dP}{dx}$.

The right-hand side of equation (5) consists of:

- $f \Rightarrow f_A = \dfrac{128\eta\Phi}{\pi D_A^4}\left(a + b\,\mathrm{Re}_A\right)$
- $u \Rightarrow u_A = \dfrac{4\Phi_0}{\pi D_A^2}$
- $c \Rightarrow c_A = \sqrt{\dfrac{D_A}{2\rho}\dfrac{1}{\left(dD/dP\right)_A}}$

Subsequently, the parameters that depend on the position, x, are:

- $\mathrm{Re} \Rightarrow \mathrm{Re}_A = \dfrac{4\rho\Phi}{\eta\pi\left(\dfrac{D_A}{2}\right)}$
- $D \Rightarrow D_A = D\left(P_{tm}^A\right)$
- $\dfrac{dD}{dP} \Rightarrow \left.\dfrac{dD}{dP}\right|_A = \dfrac{d}{dP}D\left(P_{tm}^A\right)$

As we can see the derivative $\dfrac{dP}{dx}$ can be computed for a given P_{tm}, since $\left.\dfrac{dD}{dP}\right|_A = \dfrac{d}{dP}D\left(P_{tm}^A\right)$ and $D\left(P_{tm}^A\right)$ are constitutive properties. So by starting from P_A we can compute the local derivative at A. After that we choose a sufficiently small ΔP step (so that $\Delta P = dP$) and solve for the required dx step from $x_A = 0$, or in mathematical terms:

$$\frac{dP}{dx} = \frac{-f}{1-\dfrac{u^2}{c^2}} = M,$$

where M is the local value of the derivative.

$$dx = \frac{dP}{M} \Rightarrow\ x_1 = x_A + \frac{dP}{M}$$

Finally, the process is repeated with the new starting point being $P_1 = P_A + dP$.

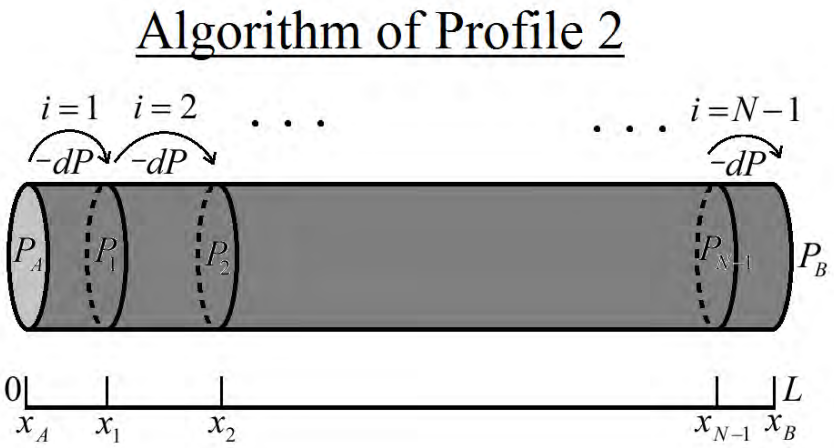

This way of calculating the profile is more efficient, since no convergence method is required. Another important difference between the 2 algorithms is that on the one hand *Profile_1* discretes the length L at $N \cdot dx$ and returns the resulting pressure P, on the other hand *Profile_2* discretes the pressure distance into smaller steps of dP and the result is the distance x from the inlet of tube.

Results of Profile_2

The main focus of Profile_2 is to check if its solution differs from the Profile_1, especially for the problematic cases we analyze previously. For this purpose, we present the solution for the same parameters as in Profile_1's example. The new solution is plotted on *Figure 4.2.4*

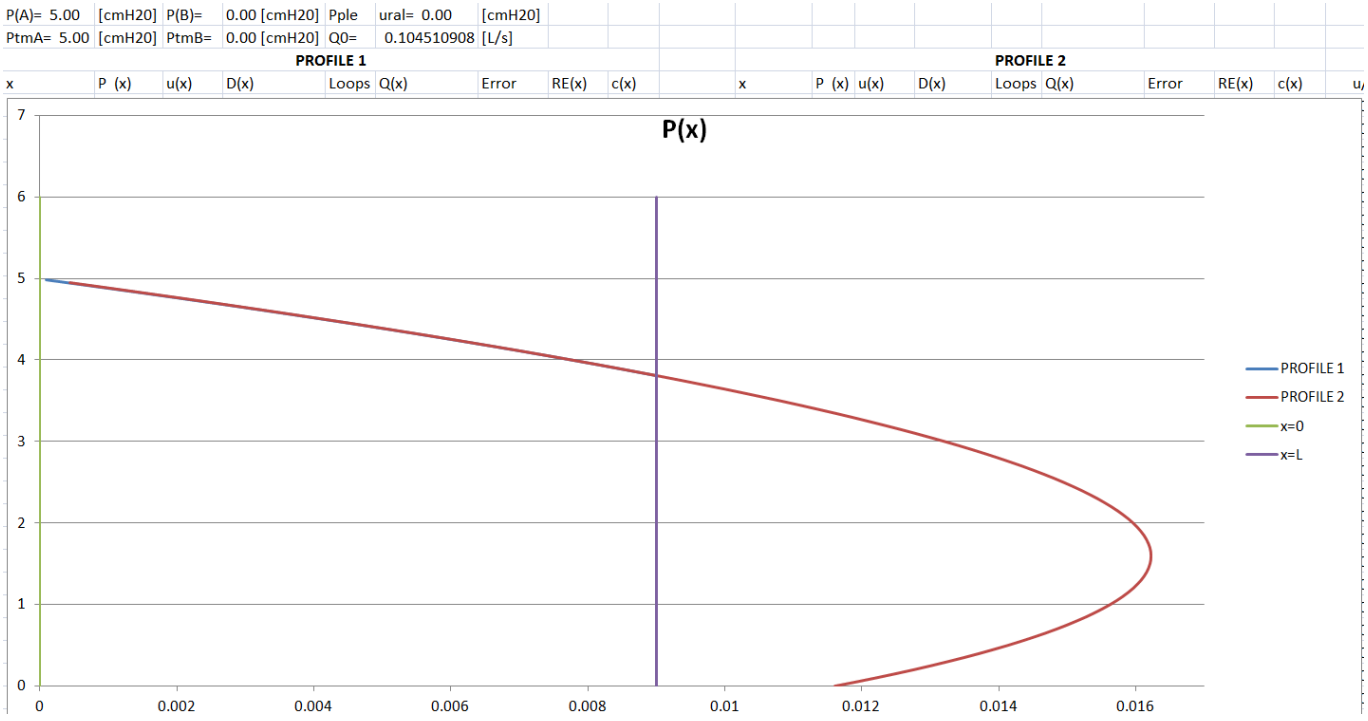

Figure 4.2.4: Problematic solution of Profile_2 of $P(x)$ *with a set of* $\{P_A = 5\, cmH_2O$, $P_B = 0\, cmH_2O, P_{pleural} = 0\, cmH_2O$, $L = 0.009\, m\}$ *,. The blue line of Profile 1 is under the red line of Profile 2.*

This profile is also problematic but reveals more about the explanations of this error. To begin with, the solutions of both Profile 1 and 2 are identical in the range $x \in (0, L = 0.009)$.

For $x > L$ it is irrational to get any values of pressure, but Profile_2 does. Since we determine the pressure P as input and calculate the distance x with this method, we force the pressure curve to be continuous from 5 to $0\, cmH_2O$. This exposes the inability of the model to give us feasible solution for some cases, via irregularities of x. A behavior like this suggests that the solution is not unique because for a given x (bigger than L) we have 2 values of P at that point.

At some point ($x \approx 0.016$) the curve changes direction and continues backwards, so the local dx is negative. The last but the most crucial observation is hiding in the differential we solve.

$$(5) \Rightarrow \frac{dP}{dx} = \frac{-f}{1-\frac{u^2}{c^2}} \Rightarrow dx = \frac{dP}{-f}\left(1-\frac{u^2}{c^2}\right)$$

Because, we know that $dP < 0$, $f \geq 0$, $u > 0$ and $c > 0$, we can continue and calculate the conditions under which $dx > 0$.

$$\Rightarrow \frac{dP}{-f}\left(1-\frac{u^2}{c^2}\right) < 0 \underset{f>0}{\overset{dP<0}{\Longrightarrow}} \left(1-\frac{u^2}{c^2}\right) < 0 \Rightarrow \left(\frac{u}{c}\right)^2 > 1 \Rightarrow \frac{u}{c} > 1$$

$$\Rightarrow u > c$$

The equation (5) seems to have a mathematical limit of $\frac{u}{c} < 1$ that needs to be explored further. But firstly, we have to examine the values of that ratio for more cases. Again we solve parametrically (by changing the quantities P_B and $P_{pleural}$) but this time the computations are made for ratios $\frac{u_A}{c_A}$ and $\frac{u_B}{c_B}$ at the inlet and outlet respectively of every tube.

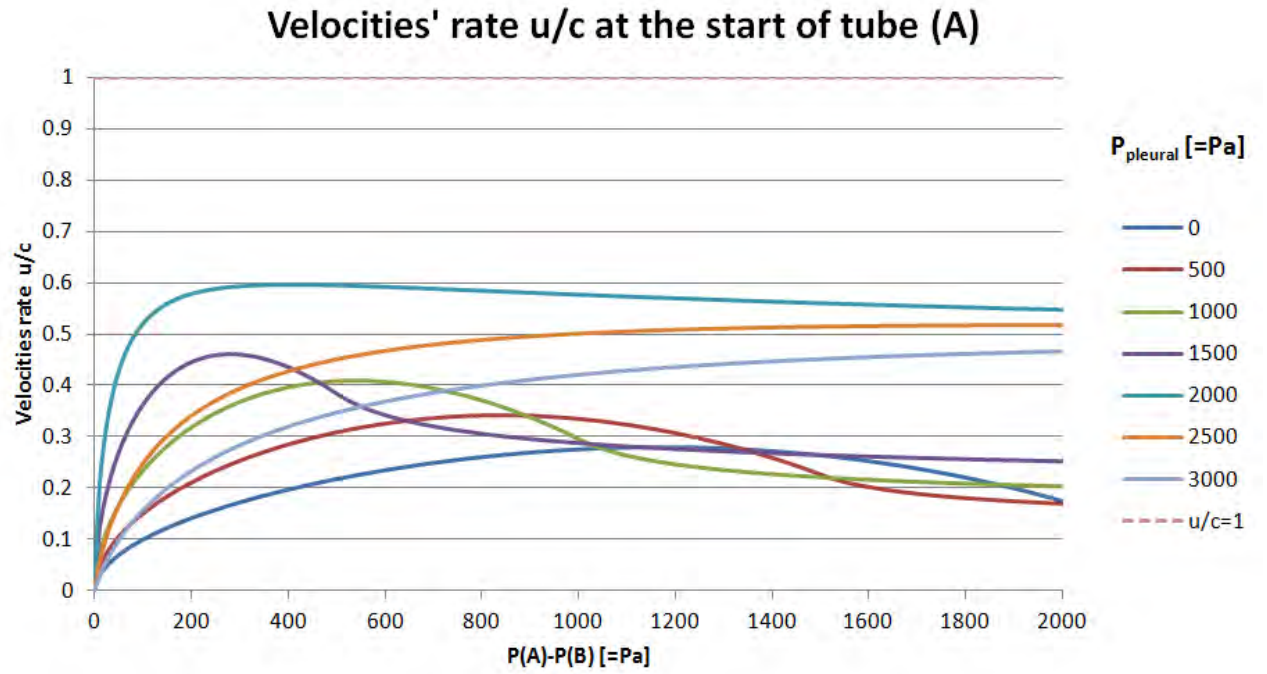

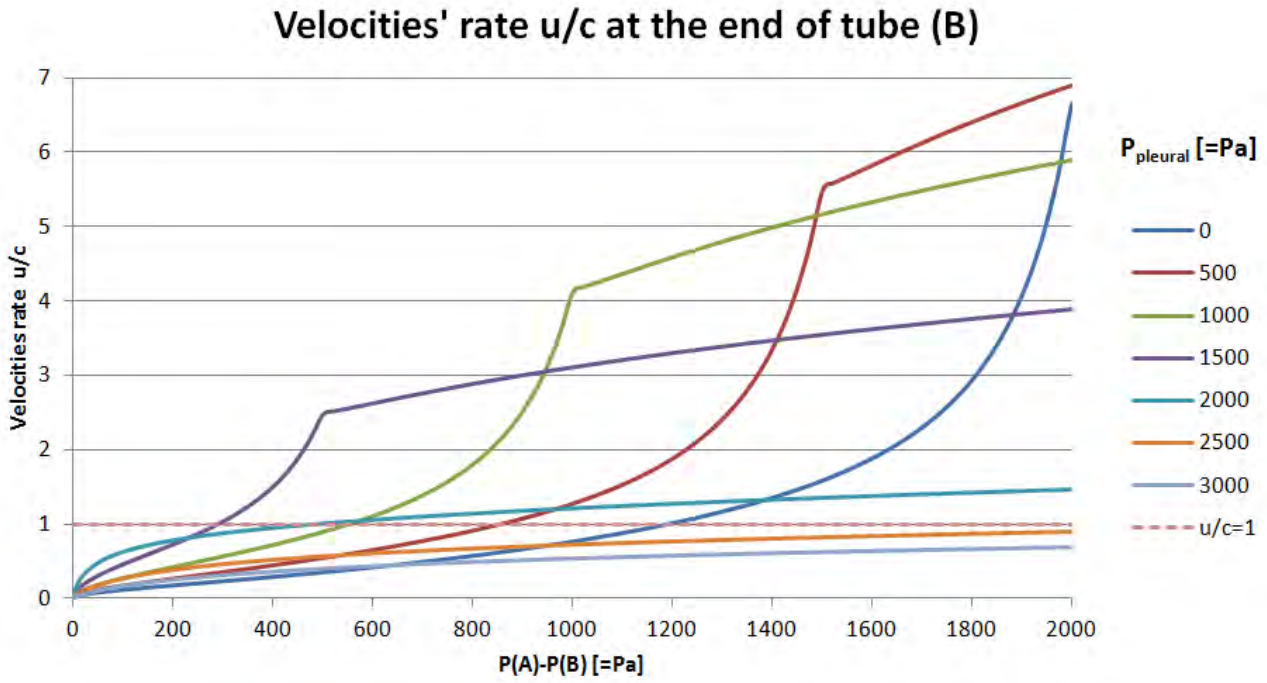

Figures 4.2.5 - 4.2.6 : Variation of velocity rate at point A and point B with a set of $\{$

$$P_A = 2000\ Pa\ , P_B = 2000 - 0\ Pa\ \}$$

It becomes clear from these 2 graphs, that the condition of $\frac{u}{c} < 1$ is violated only at the exit point B of some tubes and there are lots of cases that this violation occurs.

Next, those data lead us to test a number of profiles. We check the profiles for some cases with a $\frac{u_B}{c_B} < 1$ and some others with $\frac{u_B}{c_B} > 1$. The results showed that there is a relationship between problematic profile behaviors and the ratio of velocities at B. More specifically, when $u_B \geq c_B$ the profile fails.

4.3 The correction Φ=cA

Considering the above, we tried to find out a solution which will be able to give us answers when the ratio $\frac{u_B}{c_B} \geq 1$. The correction that arises as a solution, comes from the enforcement of the air velocity to not exceed the wave propagation speed along the tube. As we already explain, this is a reasonable assumption mathematically. The velocity of air gets a maximum value equal to wave propagation speed at every point. From this restriction, we can calculate a maximum limit for Φ inside a tube. The flow rate at any point of the tube have to be equal to $\Phi = u \cdot A$. According to the above, the condition $u = c$ results in the maximum restriction of the flow $\Phi_{\max} = c \cdot A$, where $c = c(D)$ and $A = A(D) = \frac{\pi D^2}{4}$. This is a limit that cannot be exceeded at any point of the flow. But at the same time the airflow must be constant through the whole tube, due to the conservation of mass.

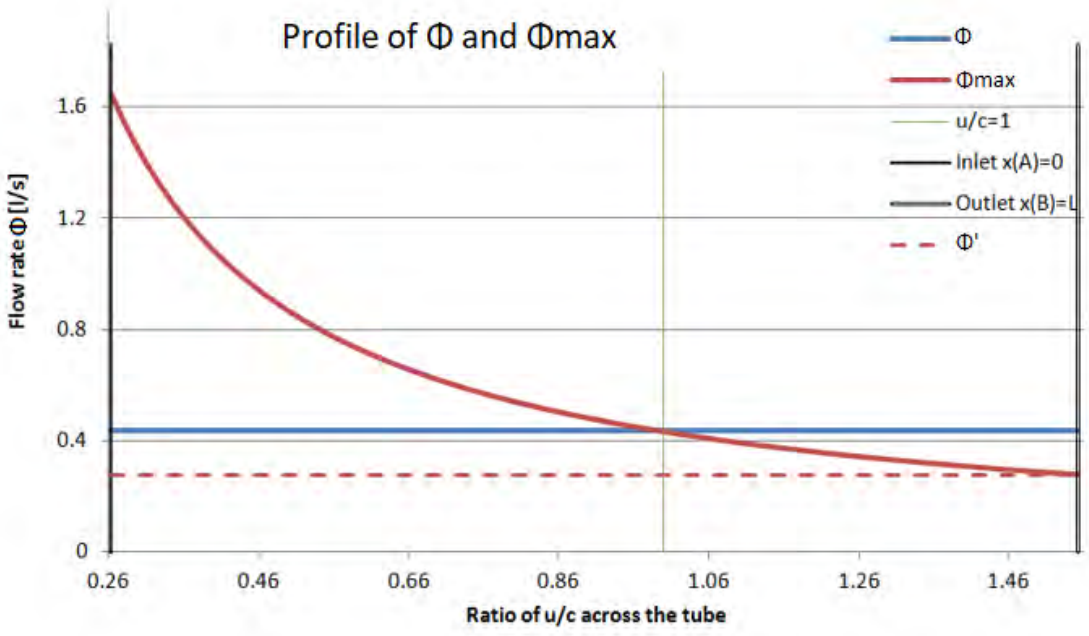

Figure 4.3.1: A plot of flow rate Φ *versus* $\frac{u}{c}(x)$ *across a tube with parameters* $P_A = 2000\ Pa$, $P_B = 500\ Pa$, $P_{pleural} = 0\ Pa$, $L = 0.009\ m$.

In *Figure 4.3.1* , we can observe the change of the restrictive $\Phi_{\max}$ along the tube for a case where the $\frac{u}{c} = 1$ was reached at some point x. The blue line represents the constant flow Φ that comes from the equation (8) (Filoche's model). After the point the two lines intersect, the limit of maximum airflow is violated, since Φ is higher than $\Phi_{\max}$. The function of $\Phi_{\max}(x)$ is strictly decreasing in every set of parameters. So the lowest value of $\Phi_{\max}(x)$ always appears in the outlet of the tube (at point B).

A proposal that partially solves the problems is to satisfy simultaneously those 2 restrictions ($\Phi < \Phi_{\max}$ and $\Phi(x) = \Phi = constant$) by changing the computational model with a condition. When a calculated flow exceeds the flow restriction $\Phi < \Phi_{\max}$ at any point (and consequently at outlet B) we will recalculate the flow as $\Phi = \Phi_{\max}(\mathrm{B}) = \mathrm{c}_B \cdot A_B$ since it is the lowest feasible value (Φ' at *Figure 4.3.1*), but otherwise Φ remains the same (equation (8)).

The relation for Φ that applies with the modified model is:

$$\Phi = \begin{cases} (8) = \dfrac{\sqrt{k^2 - 4jl} - k}{2j} & , \quad if \quad (8) < \Phi_{\max} \\ (9) = c_B \cdot A_B & , \quad if \quad (8) > \Phi_{\max} \end{cases} \qquad (10)$$

In other words, the resulting Φ from equation (8) (Filoche's model) is checked for the case that Φ exceeds $\Phi_{\max}(\mathrm{B})$. When this violation occurs the Φ is again computed from the simplified equation (9). In a way, this model forces the flow to get maximum speed c always at point B and because the ratio $\frac{u}{c}$ strictly increases along the tube we are not getting ratios $\frac{u}{c} \geq 1$ before point B.

It is worth noting that equation (9) is a very simplified model and the pressure $P_{tm,B}$ is the only unknown variable to determine the Φ value, since $c_B = c\left(P_{tm,B}\right)$ and $A_B = A\left(P_{tm,B}\right)$.

Results

This correction is added to the computational process and then a new parametric analysis was made. The previous and new results are merged in a single diagram for comparison between the 2 approaches.

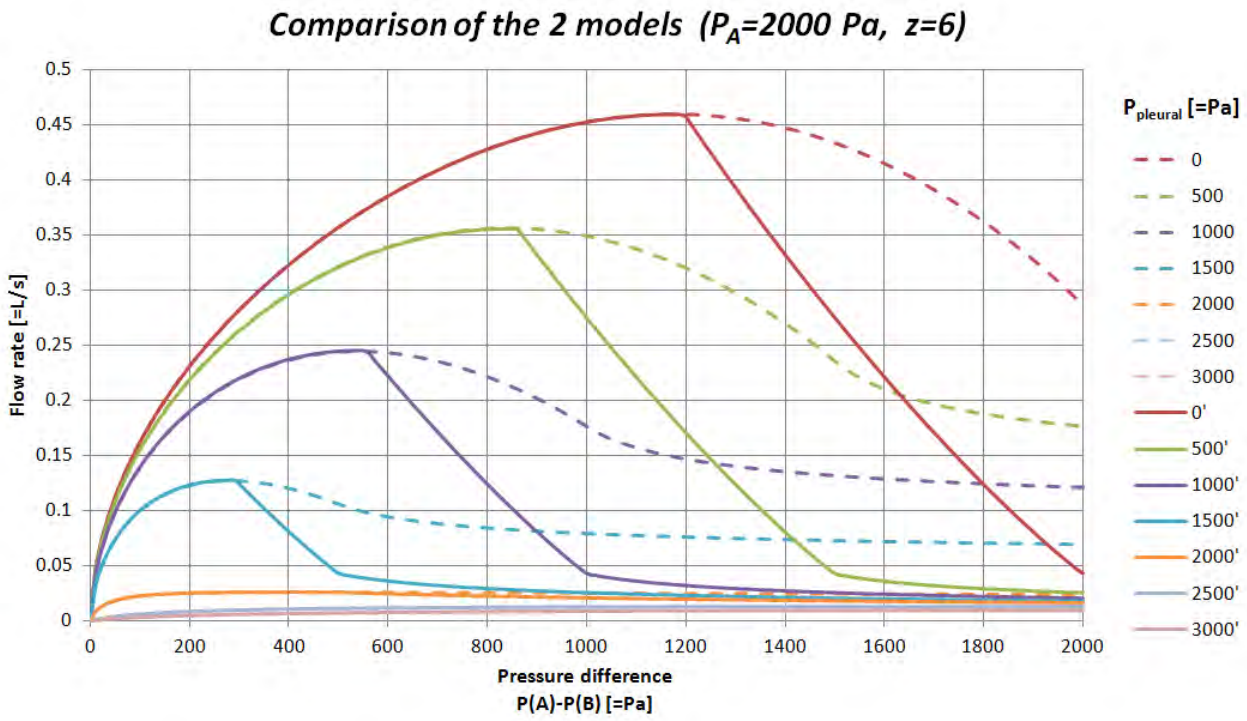

Figure 4.3.2: Graph $\Phi - \Delta P$ *- parametrically for* $P_{pleural}$ *, where the dotted lines corresponds to the initial model from equation* (8) *and the continuous lines to the modified model from equation* (10)

As a quick reminder, the concept of the parametric analysis is to present with a condensed way the resulting flow rate for many different pressure scenarios on the boundaries of a tube. Each curve is defined from a specific external pressure field and each point on it has a different driving force ΔP across the channel.

The new curves which are created provide different results above the maximum point Φmax in each generation. The next question that arises is which of the two models approach more accurately the actual behavior of the tube.

It's easy to observe that the curves afterward applying the correction $\Phi = cA$, converge into the same minimum value Φ_{min} without affected by the size of pleural pressure. This result, however, doesn't correspond to our intuition, as we expected the tubes with greater external pressure to provide smaller amounts of flowrates by setting the same pressure drop. Bearing this in mind and comparing the two models and their curves, we realized that the first determination of *Filoche* confirms the above thought which leads us to consider that *Filoche's* model is more acceptable.

5. The mechanism of flow limitation

It has been clear that whenever the velocity of air approaches the wave propagation speed the model of *Filoche* isn't able to predict the behavior of the tube. According, also, to *S.V. Dawson* and *E.A. Elliott (1977)* this condition leads to a phenomenon which appears only in elastic tubes and is known as ''flow limitation''. It has been referred also in chapter 1 as the basic mechanism of Starling Resistor. So, in this chapter we are trying to describe in more detail this mechanism and giving explanations about the relation between human forced expiration. The chapter ends presenting a more explicit and alternative depiction of flow limitation as a waterfall.

5.1 Introduction to flow limitation

In rigid and fixed diameter tubes, the value of flowrate variates proportionally with pressure drop ($\Phi - \sqrt{\Delta P}$). This, however, doesn't happen in tubes with deformable walls such as bronchioles. Due to constant drop of airway pressure and the act of external pleural pressure, the cross-section area narrows. Especially, in deeper and more compliant generations this variation is more intense. As a result, the velocity of air gets increasingly greater values in order to balance the value of flowrate and satisfy the equilibrium of mass. According to this, it is possible in some point the air velocity to increase so much that reaches the wave propagation speed. There, the flow becomes limited causing the partial collapse of tube wall *Figure 5.1.1*

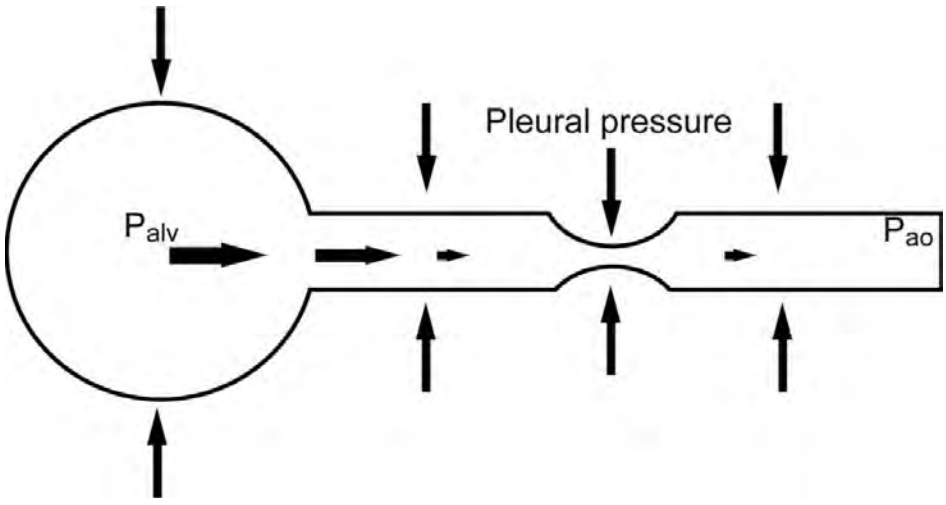

*Figure 5.1.1: The collapse of bronchiole (*http://rc.rcjournal.com/content/62/9/1212/tab-figures-data)

The narrowest point where flow limitation occurs is called ''choke point'' and defines the critical pressure drop in which flowrate gets the maximum value (Φ_{max}). Above that point the flowrate remains

constant despite possible increases in driving pressure. This effect has been observed from the curves we got in chapter 4, solving parametrically the Bernoulli equation in which after a specific point, an increase in pressure drop ($P_A - P_B$) didn't affect the value of flowrate *Figure 5.1.2.*

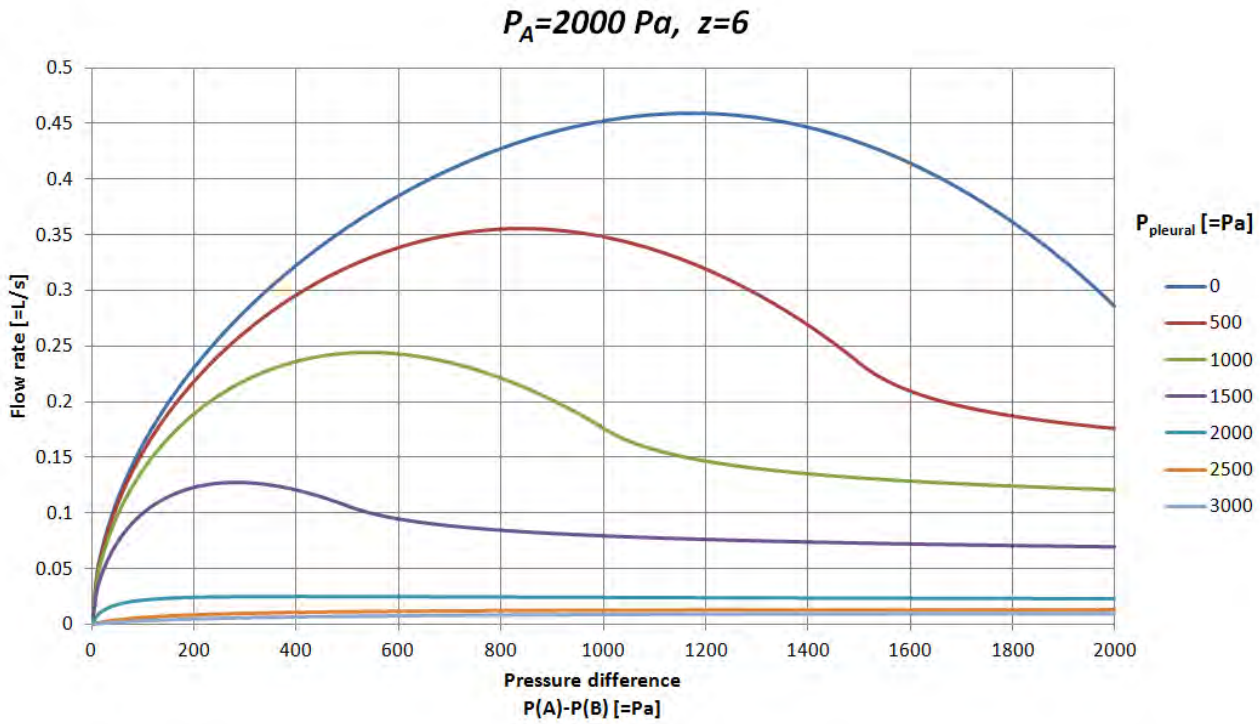

Figure 5.1.2: ''Flow limitation'' is more clearly in the curves which have greater pleural pressure $(P_{pl} = 2000, 2500, 3000)$ *where after a small pressure drop the value of flowrate is constant.*

5.2 Forced expiration

This phenomenon is observed also in forced expiration. At first, forced expiration is an exhalation procedure that is accomplished with a fast and strong release of air that preceded by deep inspiration from nose or mouth. In medicine, this value of forced flowrate can be measured and is extremely useful in pulmonary function tests (spirometry) as it checks the condition of the lungs, *Figure 5.2*

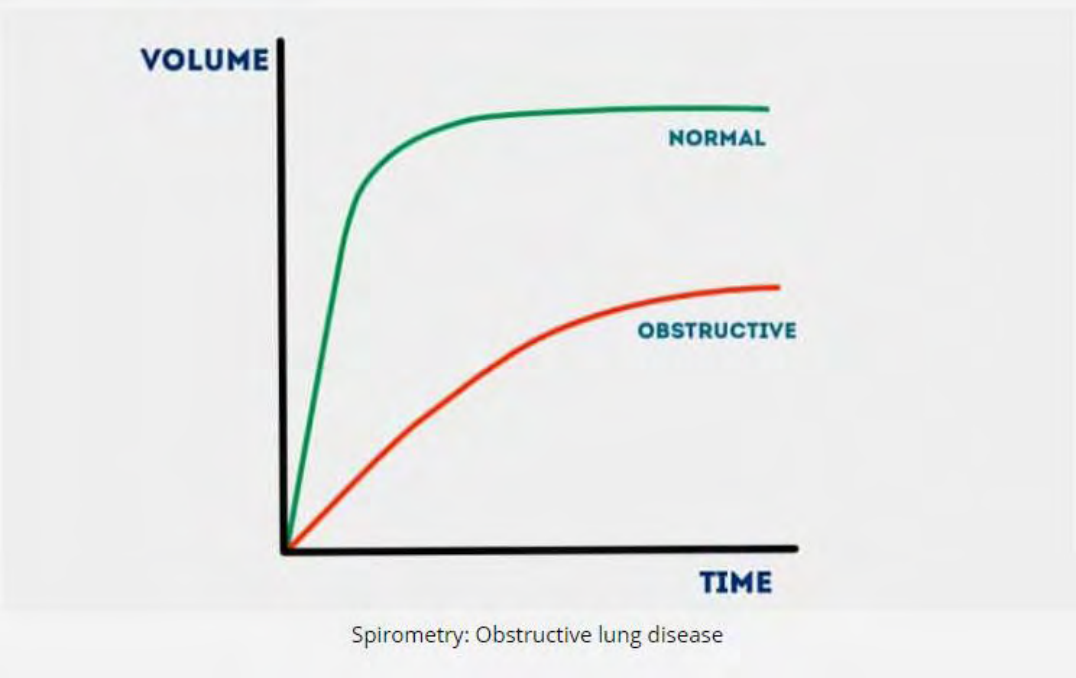

*Figure 5.2: A Comparison between normal and obstructive lung (*https://geekymedics.com/spirometry-interpretation/)

During forced expiration the contraction of expiratory muscles increase pleural pressure P_{pl}. This causes two opposing effects:

- It increases the upstream driving pressure P_A inside alveoli which tend to increase flowrate
- It leads bronchioles to narrow even more increasing this way the resistance of the flow due to friction forces.

According to Bernoulli's principle and *Lambert* notes the total energy of air in some point before choke point is determined from the total energy in alveoli $P_A + \frac{1}{2}\rho u_A{}^2$ reduced by the total friction losses $\int_0^x f(y)dy$. As the airway narrows the term of friction losses increases and a part of lateral pressure (P) converts into dynamic pressure ($\frac{1}{2}\rho u^2$). The interaction between these two components (friction losses and dynamic pressure) lead to strong loses of lateral pressure and as soon as air velocity reaches the wave propagation speed flow limitation is produced *(World Congress of Medical Physics and Biomedical Engineering 2006)*. Further increases in effort (i.e. blowing more forcefully) will not affect the value of flowrate cause the narrowing depends on the surrounding pleural pressure Ppl. The transmural pressure will not be affected because the intra-airway pressure is increased by the same

amount of pleural pressure does. So, the difference between inside and outside pressure will be the same as before.

5.3 The analogy of waterfall

This independent relation between pressure drop-flowrate and in general the flow limitation mechanism present similar behavior as a flow in a waterfall *(Wagner,1994*), *Figure 5.3*

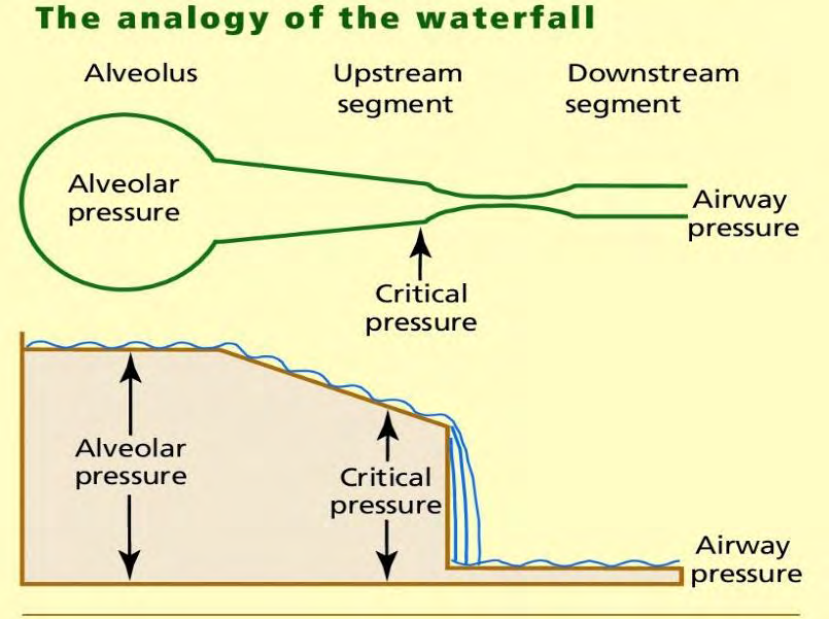

*Figure 5.3 : Flow limitation as a waterfall (*https://www.researchgate.net/publication/7570845_Auto-positive_end-expiratory_pressure_Mechanisms_and_treatment)

The flowrate in a waterfall depends on the altitude difference between upstream pressure and the edge of waterfall. The downstream pressure which is determined from the height of waterfall can't affect the flowrate at the top. This parallels the case of flow limitation where the pressure difference between alveoli and airway pressure ends cannot influence the flowrate. In other words, the airflow is determined from the gradient of alveolar pressure and critical pressure (''choke point'') and not from downstream pressure. So, increasing the pressure drop (effort) is even as increasing the height of the waterfall.

6. Outline of more detailed modeling

As we are trying to explore further the model of Filoche and Florence and its limits, we realize that whenever the mechanism of flow limitation occurs the prediction of pressure along the tube is not so simple. The reason seems to be that the basic assumptions which have been made in *Filoche's* model, cease to exist affecting critically the flow and the general results of Bernoulli's principle. In this section we discuss these assumptions and how they may be relaxed as flow limitation develops. More specifically, we touch on three issues: multi-dimensional effects, non-cylindrical tube collapse and time-varying phenomena.

The analysis of Filoche and the simplification of it, is based remarkably on the assumption of one-dimensional flow. More specifically, the value of velocity and pressure in all numerical processes was depended only on the position along the tube. Even though this assumption is reasonable in most cases and leads to physically acceptable results, in the case of flow limitation the behavior becomes more complicated. Considering as known the geometry of bronchiole, the general effect is similar to the flow in a rigid tube with a converging and a diverging section, *Figure 6.1.*

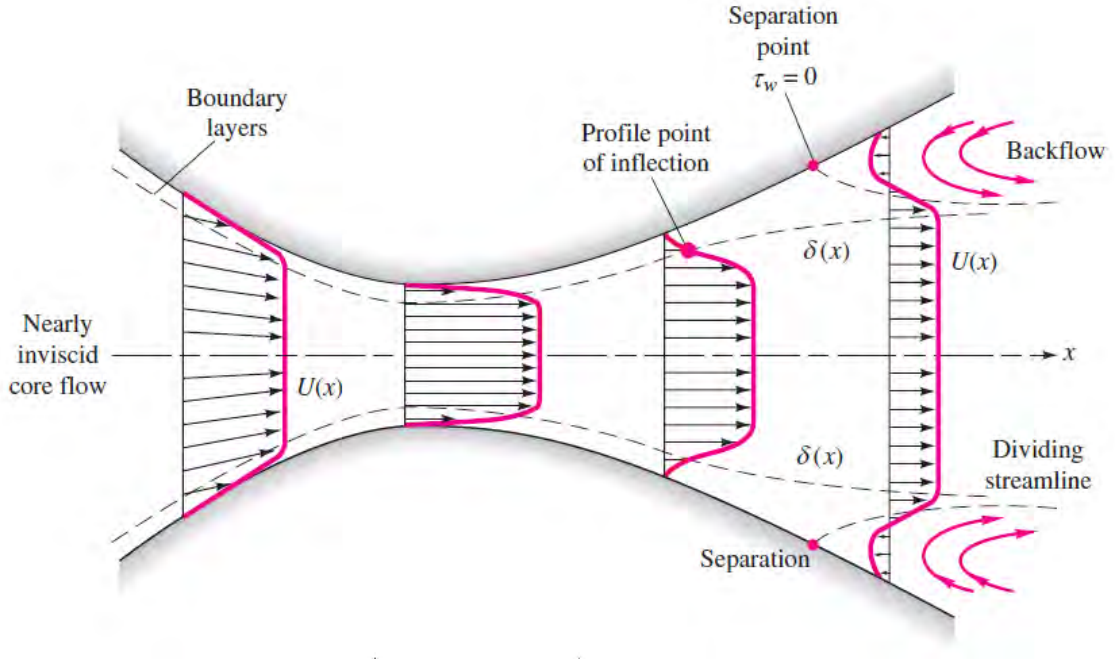

Figure 6.1: The velocity profile $U(x)$ in a nozzle-diffuser configuration

As we can notice, before the throat area, the flow is uniform and the boundary layer doesn't separate. The reason is because the direction of the flow agrees to the decrease of static pressure (favorable gradient). However, as the air passes the throat the expanding area forces a constant deacceleration,

increasing this way its static pressure (unfavorable gradient or adverse pressure gradient). If the diffuser's angle is too large it increases the disturbed flow and leads to a more evident boundary layer separation. This detachment forms backflows which increase energy losses and they have to be included in overall analysis. The above scenario could lead to a throat that moves towards the inlet with increasing air flow rate.

A consequence of flow limitation, which referred also in previous chapter, is the collapse of the elastic tube. Due to the prevailing conditions inside and outside, the tube wall isn't able to hold a circular cross-section area. The shape of airway varies in a different way *(Grotberg, Jensen ,2014) Figure 6.2.*

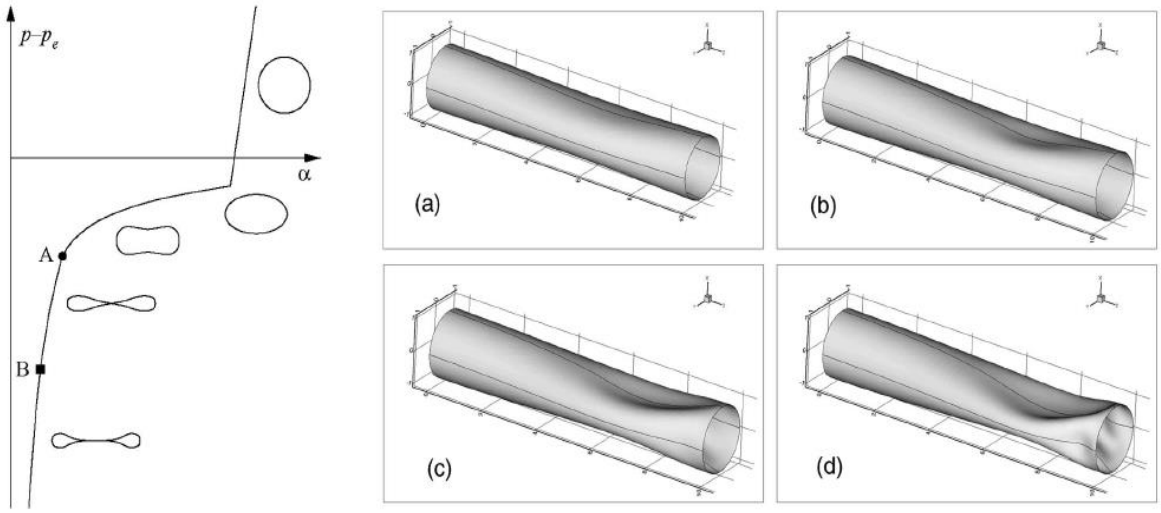

Figure 6.2: Different shapes of cross section area as the transmural pressure drops

Experiments which made in Starling resistor showed the above views of surface. For $P_{tm} = P - P_e > 0$ the tube is fully inflated and the area circular. As the transmural pressure becomes slightly negative the elastic tube tend to form an elliptical cross section area depending on tube stiffness. If the transmural pressure drops even more the tube collapses and it can lead to the contact of opposite walls. In lungs this complete collapse of the walls can occur in smaller diameter and thicker walled bronchioles *(Bertran, 1987)*. So, in choke point and above it, this phenomenon is more intense and a consideration of circular cross section $A = \pi * D^2 / 4$ seems to lead to inaccuracies.

Moreover, self-excited oscillations which can be observed in the flutter of flags in the wind or in the wings of airplane whenever a critical speed is exceeded appear also in forced expiration. Experimental studies *(Luo, Pedley, 1996)* have shown that flows with high Reynolds number and large deformations of elastic tube wall can cause large amplitude self-exited oscillations. They arise from the energy

transfer of the fluid into the elastic wall which is accompanied with an expansion of it. These oscillations influence the analysis and the equations that govern it, demonstrating that the time dependent terms cannot be neglected.

A one-dimensional model that describes these unsteady conditions for the case of blood flow has been described by *Larson, Bowman, Papadimitriou, Koumoutsakos, Matzavinos (2019).:*

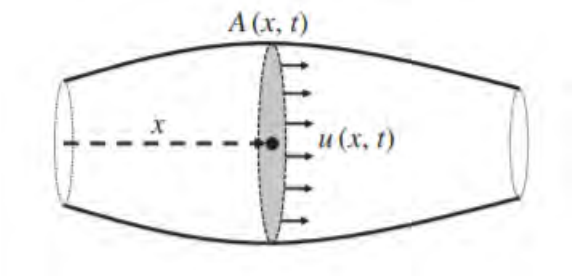

Figure 6.3: Schematic of one-dimensional and time-varying artery

The partial differential equations that have been produced are derived from the conservation of mass and momentum/Navier-Stokes, assuming viscous, incompressible and 1-D axial direction flow:

$$\left.\begin{aligned} \frac{\partial A}{\partial t}+\frac{\partial (Au)}{\partial x}&=0 \\ \frac{\partial u}{\partial t}+u\frac{\partial u}{\partial x}&=-\frac{1}{\rho}\frac{\partial p}{\partial x}+K_r\frac{u}{\rho A}, \end{aligned}\right\}$$

Here, ρ is the flow density and K_r is a parameter representing viscous resistance per unit length, given by $K_r=-22\mu\pi$ in terms of the viscosity μ of blood and the chosen velocity profile.

Conclusions

This paper achieved some of its primary goals. More specifically:

- the presentation of interesting biological and industrial systems where flexible pipes are applied
- the development of constitutive equations which relate the transmural pressure to the diameter and the mechanical properties of elastic tubes
- the construction process of Filoche's model explaining it and building it from the general mass and energy equilibrium in an open system
- the calculation of flowrate for a different set of parameters and the production of curves that reflect not only this variation but, also, the phenomenon of ''flow limitation''
- our effort to extend the analysis in order to provide detailed results about the pressure drop in a tube, and the problems we faced with un-realistic solutions due to flow limitation
- a more detailed description of flow limitation and the consideration of effects that were neglected in the analysis

Recommendations for future work

This thesis stigmatized from a sort of issues that took a lot of time to understand and it would be interesting, despite the complexity, to be presented in a future research:

- a research for a different model that corresponds to flow limitation and the effects that follow, in order to receive acceptable results for the variation of pressure in a single airway
- a further investigation about the results of this thesis, each one has its own interest, to explain more clearly the consequences of flow limitation
- a calculation of airflow using analytical tube models as presented in table 1 and a comparison between Lambert's model

References

Bai Q., Bai Y., Ruan W., 2017, Advances in Pipes and Pipelines: Flexible Pipes, Part I Design and analysis, 3-13

Calder I., Pearce A., 2011, Core Topics in Airway Management, 22-25

Carpenter P.W., Pedley T.J., 2001, Flow Past Highly Compliant Boundaries and in Collapsible Tubes, Chapter 2 Flows in deformable tubes and channels, 15-49

Elliot E.A., Dawson S.V.,1977, Wave-speed limitation on expiratory flow- a unifying concept, Test of wave-speed theory of flow limitation in elastic tubes, 516-522

Filoche M., Florens M., 2011, Journal of Physics: Conference Series 319, The stationary flow in a heterogeneous compliant vessel network

Giamagas G., Monokroussos N., 2018, Integrated computational simulation of the mechanics of breathing

Grotberg J.B., Jensen O.E., 2004, Biofluid Mechanics in Flexible Tubes, 121-135

Hamid Q., Shannon J., Martin J., 2005, Physiologic basis of respiratory disease, Chapter 6 Physics of expiratory flow limitation, 55-60

Hayashi K., Ishikawa H., 1996, Computational Biomechanics, Numerical Analysis of Flow in a Collapsible Vessel Based on Unsteady and Quasi-Steady Flow Theories,

Katz A.I., Chen Y., Moreno A.H., 1969, Biophsyic Journal, Volume 9, Flow through a collapsible tube, 1261-1279

Lambert R.K., Wilson T.A., Hyatt R.E., Rodarte J.R., 1982, A computational model for expiratory flow, 44-56

Larson K., Papadimitriou C., Koumoutsakos P., Matzavinos A., 2019, Detection of arterial wall abnormalities via Bayesian model selection, 1-4

Morgan P., 1985, Unsteady flow in collapsible tubes, Chapter 1 Introduction and applications, 10-14

Paidoussis M.P., 1988, Fluid-structure interactions slender structures and axial flow, Chapter 1 Cylindrical Shells Containing or Immersed in Flow: Advanced Topics and Applications, 95-135

Polak A.G., Mroczka J., 2006, World Congress of Medical Physics and Biomedical Engineering 2006, Analysis of flow limiting mechanisms during forced expiration, 87-88

Schwartzstein R.M., Parker M.J., 2006, Respiratory Physiology A Clinical Approach, Chapter 4 Dynamics: Setting the system in motion, 69-90

White F.M., 2011, Fluid Mechanics, Seventh edition, Chapter 7 Flow past immersed bodies, 476-482

[1] https://en.wikipedia.org/wiki/Peristaltic_pump

[2] https://www.urotoday.com/urinary-catheters-home/history-of-urinary-catheters.html

[3] http://hdl.handle.net/1721.1/109244

[4] https://hal.archives-ouvertes.fr/hal-01807385/document

[5] https://www.researchgate.net/publication/7570845_Auto-positive_end-expiratory_pressure_Mechanisms_and_treatment

[6] http://rc.rcjournal.com/content/62/9/1212/tab-figures-data

[7] https://geekymedics.com/spirometry-interpretation/

Appendix: Program (Elastic_tube) for the calculation of airflow Φ and the pressure profile P(x) during the breathing procedure using *Lambert's* parameters.

Depending on the value of variable Option, the main part of program can call 3 basic subroutines (Parametric_analysis, Profile_1, Profile_2) in order to calculate the flowrate or the profile. The algorithm of the main part is given below:

```
Program Elastic_tube
!*****************************************************************************************************************
!This program simulates the air flow throught a cylindrical elastic pipe with external pressure,
!   using the Lambert's model as constitutive equation for the walls that describes the deformation
!   of human lung airwais under tension. It can run with 2 different options, depending on the value
!   of variable "option":
!* Option=1 : For a given range of P(B) and P_pleural, computes the flow rate Q for every combination
!   of P(B) and P_pleural and types it on file "Prametric_analysis.txt" (Subroutine Parametric_analysis).
!* Option=2 : In this option, P(A),P(B) and P_pleural are the inputs, and the resulting flow rate Q is
!   calculated (Subroutine "PressureFlow"). After that with a converging process the profile along x-axis
!   of diameter, velocity and pressure is computed.
!*****************************************************************************************************************

    implicit none

    integer z, x_nodes, sum1, sum2, n, i, option
    real*8, parameter :: pi=dacos(-1.D0)
    real*8 P_A, P_B, P_pl, PtmA, PtmB, D_A, D_B, a_A, a_B, h_A, h_B, L, a0, a0_, n1, n2, Am, Dmax, P1, P2
    real*8 A, B, C, Delta, alpha, beta, Re, Re_A, Re_B, Q, Q_2, Qmax, u_A, u_B, R_aver, x, dx, diff
    real*8 dP_0, dP_B, P_B_max, P_0_max, PB, Ppl, Q_Pois, Q_max, p, N_t, P_ave, Ru, T, ro, ita, ni
    real*8 PtmX, start, finish, Dk, Lk, u_cA, u_cB
    real*8 T_a0(17), T_a0_(17), T_n1(17), T_n2(17), T_Am(17), T_L(17), T_Dk(17), T_Lk(17)

    !-Open necessary files
    open(10,File="Data.txt", Status="Old")
    open(11,File="Airway_curves.txt", Status="Unknown")
    open(12,File="Results.txt", Status="Unknown")
    open(20,File="Profile_1.txt", Status="Unknown")
    open(30,File="Profile_2.txt", Status="Unknown")
    open(40,File="Parametric_analysis.txt", Status="Unknown")
    open(50,File="Ratios.txt", Status="Unknown")

    !-Calculates CPU running time
    call cpu_time(start)
    write(*,'("Loading...")')

    !Option= {1:for parametric analysis, 2:for profile}
    option=2

    !-Input trasmural pressures. For parametric analysis subroutine, this values are the starting ones.
    P_pl=   10.d0          ![=cm H2O]
    P_A=     9.d0          ![=cm H2O]
    P_B=     8.d0          ![=cm H2O]

    !-Iputs for parametric analysis: Range of P(B) and Ppl.
    dP_B=   0.1d0
    dP_0=   5.d0
    P_B_max= P_A
    P_0_max= 30.d0

```

```
    !-Read model parameters of bronchial mechanics from "Data.txt" file.
    read(10,*) T_a0, T_a0_, T_n1, T_n2, T_Am, T_L, T_Dk, T_Lk

    !-Calculation of parameters related to D(Ptm) and h(Ptm).
    z=6
    N_t=2.d0**z ; a0=T_a0(z+1) ; a0_=T_a0_(z+1) ; n1=T_n1(z+1); n2=T_n2(z+1) ; Am=T_Am(z+1); L=T_L(z+1)
    L=L*1.d-2       ![=m]
    PtmA=P_A-P_pl   ![=cm H2O]
    PtmB=P_B-P_pl   ![=cm H2O]

    !-Solving only for the chosen option.
    if (option==1) then
        !-Create Q - (P(A)-P(B)) graphs for different Ppl values
        call Parametric_analysis(P_B,P_B_max,dP_B,P_pl,P_0_max,dP_0)
    else if (option==2) then
        !-Ptm(A), Ptm(B) and L are the inputs, and the resulting flow rate Q is calculated.
        call PressureFlow(PtmA,PtmB,L)
        !-For this specific solution [from PressureFlow] the profiles of velocity and pressure
        ! across the tube is computed with 2 different ways.
        call Profile_1
        call Profile_2
    end if

    !-Recreation of Lambert's diagrams [α=A(Ptm)/Amax - Ptm for each generation z].
    call Curves

    !-Computing the total running time of the code.
    call cpu_time(finish)
    write(*,'("CPU running time [s] =",f16.8,/,"Press enter to close...")') finish-start
    read*

!*****************************************************************************************************************
```

Subroutine Parametric_analysis calls iteratively the subroutine PressureFlow calculating the airflow Φ for a range of P(B) and $P_{pleural}$. Also, writes the results into the ‘’Parametric_analysis.txt’’ file:

```
    Contains
!*****************************************************************************************************************

    Subroutine Parametric_analysis(P_B,P_B_max,dP_B,P_pl,P_0_max,dP_0)
    !*************************************************************************************************************
    !For given Ppleural and P(B) ranges as inputs, this subroutine calculates the flow rate [=L/s]
    !and saves the results on "Parametric_analysis.txt" file.
    !*************************************************************************************************************

    real*8 P_B, P_B_max, dP_B, P_pl, P_0_max, dP_0
    integer pB_node, pB_node_max, p0_node, p0_node_max, j

    pB_node_max= int( (P_B_max-P_B)/dP_B )
    p0_node_max= int( (P_0_max-P_pl)/dP_0 )

    write(40,'("P(A)=",f6.2,",   Generation z=",i2,", Q: L/s, Pressures: cmH20")') P_A,z
    write(40,*)

do j=1,3
    if (j==1) then
                write(40,'(" ",30x,"Flow Q [=l/s]")')
    else if (j==2) then
                write(40,'(" ",30x,"Ratio u/c at A")')
    else
                write(40,'(" ",30x,"Ratio u/c at B")')
    end if

    write(40,'("P(A)-P(B)|Ppl:    ",\)')

    do p0_node=1,p0_node_max+1
        Ppl=P_pl+(p0_node-1)*dP_0
        write(40,'(f8.2,"   "\)') Ppl*98.0665d0
    end do
    write(40,*)

    do pB_node=pB_node_max+1,1,-1

        PB=P_B+(pB_node-1)*dP_B
        write(40,'(f8.2,7x," ",\)') (P_A-PB)*98.0665d0

        !-Loops for 8 values of Ppl
        do p0_node=1,p0_node_max+1

            Ppl=P_pl+(p0_node-1)*dP_0


            !-Find mass flow rate for given pressure
            PtmA=P_A-Ppl      ![=cmH2O]
            PtmB=PB-Ppl      ![=cmH2O]

            call PressureFlow(PtmA,PtmB,L)

            !call Prints
            if (j==1) then
                write(40,'(\,f10.6," ")')  10**3*Q
            else if (j==2) then
                write(40,'(\,f10.6," ")')  u_cA
            else
                write(40,'(\,f10.6," ")')  u_cB
            end if


        end do
        write(40,*)

    end do
    write(40,*)

end do

    End subroutine
```

Subroutine PressureFlow calculates for a given pressure difference and length, the value of flowrate:

```
153
154
155     Subroutine PressureFlow(PtmA,PtmB,L)
156     !*****************************************************************************************************
157     !This subroutine computes the air flow rate for a cylindrical tube with lenght L and
158     !pressure difference PtmB-PtmA across it.
159     !*****************************************************************************************************
160
161     real*8 PtmA, PtmB, L, M, c_A, c_B
162
163     D_A= D(PtmA)
164     D_B= D(PtmB)
165     h_A= h(PtmA)
166     h_B= h(PtmB)
167
168     !-Properties of air
169     P_ave=1.d5                          ![=Pa]
170     Ru= 287.058d0                       ![=J/kg/K]
171     T= 25.d0+273.d0                     ![=Kelvin]
172     ro= P_ave/Ru/T                      ![=kg/m3]
173     ita =18.37d-6                       ![=Pa*s]
174     ni=ita/ro                           ![=m2/s]
175     alpha= 1.5d0
176     beta= 0.0035d0
177
178     !-2nd Order Equation of Q [=m3/s]
179     A=1024.d0*L*ro*beta/( (pi**2)*(D_A+D_B) ) -32*ro*log(D_B/D_A)/(pi**2)
180     B=128.d0*ita*L*alpha/pi
181     C=h_B-h_A
182
183     !-Solutions
184     Delta=B**2-4.d0*A*C
185     Q=(-B+dsqrt(Delta))/(2*A)           ![=m3/s] The positive (accepted) root
186     Q_2=(-B-dsqrt(Delta))/(2*A)         ![=m3/s] The negative (rejected) root
187
188     !Velocity [=m/s] at the outlet x=L
189     u_B=4*Q/pi/(D_B**2)                     ![m/s]
190     !Critical velocity at x=L
191     M=2*ro*dD(PtmB)/(98.0665d0*D_B)
192     c_B=dsqrt(1.d0/M)
193
194     Q_max=c_B*pi*(D_B**2)/4.d0
195     if (u_B>c_B) then
196         !Q=Q_max
197         !print*, PtmB
198         !read*
199     end if
200
201     !Velocity [=m/s] at the inlet x=0 and outlet x=L
202     u_A=4*Q/pi/(D_A**2)
203     u_B=4*Q/pi/(D_B**2)
204     !Critical velocity at x=0
205     M=2*ro*dD(PtmA)/(98.0665d0*D_A)
206     c_A=dsqrt(1.d0/M)                           ![m/s]
207     !Critical velocity at x=L
208     M=2*ro*dD(PtmB)/(98.0665d0*D_B)
209     c_B=dsqrt(1.d0/M)                           ![m/s]
210     !Ratio u/c at points A and B
211     u_cA=u_A/c_A   ;  u_cB=u_B/c_B
212
213
214     !Reynolds numbers: at the inlet x=0, outlet x=L, and for the average diameter of D(x)
215     Re=(4*Q)/(ita*pi*(D_A+D_B)/2.d0)
216     Re_A=ro*u_A*D_A/ita
217     Re_B=ro*u_B*D_B/ita
218
219     !-Ideal maximun flow rate (Poiseuille flow)
220     R_aver=(D_A+D_B)/4.d0
221     Qmax=dsqrt(2.d0*(98.0665d0*(PtmA-PtmB))/ro) * ( R_aver**2 )*pi       ![=m3/s]
222     Q_Pois=-( (98.0665d0*(PtmB-PtmA))*pi*(R_aver)**4 ) / (8*ita*L)       ![=m3/s]
223
224     call Prints
225
226     End subroutine
```

Functions D(P), dD(P), h(Ptm) compute the diameter of the elastic tube, the derivative of diameter and the integral of $D^4(P_{tm})$ which are necessary variables for the calculations:

```
227
228
229     Real*8 function D(P)
230     !*****************************************************************************************************
231     !This function computes the diameter of the pipe for a given transural (internal-pleural) pressure
232     !using Lambert's model arising from experimental data that describes the deformation of lung airways.
233     !*****************************************************************************************************
234
235     real*8 P,alfa,A
236
237     !-Parameters of D(Ptm) and h(Ptm)
238     Dmax=2.d0*dsqrt(Am/(N_t*pi))    ![=cm]
239     Dmax=Dmax*1.d-2                 ![=m]
240     P1=a0*n1/a0_                    ![=cmH20]
241     P2=-n2*(1-a0)/a0_               ![=cmH20]
242
243         If (P<=0.d0) then
244             alfa=a0*(1.d0-P/P1)**(-n1)
245         else
246             alfa=1.d0-(1.d0-a0)*(1.d0-P/P2)**(-n2)
247         end if
248         A=alfa*Am/N_t
249         D=Dmax*dsqrt(alfa)
250
251     End function
252
253
254     Real*8 function dD(P)
255     !*****************************************************************************************************
256     !This function calculates the derivative dD(P)/dP, using a second order central numerical method.
257     !*****************************************************************************************************
258     real*8 dP, P_r, P_l, P, P_2r, P_2l
259
260     dP= 0.1d0
261     P_r= P+dP
262     P_2r=P+2*dP
263     P_l= P-dP
264     P_2l=P-2*dP
265     dD=( -D(P_2r)+8*D(P_r)-8*D(P_l)+D(P_2l) )/(12*dP)
266
267     End function
268
269
270     Real*8 function h(Ptm)
271     !*****************************************************************************************************
272     !Parameter h [=N*m2] is a function of Ptm and equal to h(P)=integral of[D(P)^4]dp from 0 to P.
273     !The integration is calculated numerically using the simplest method, the trapezoid rule.
274     !*****************************************************************************************************
275
276     real*8 Ptm, dh, f_p, p, diff, n, i, sum
277
278     !-Numerical integration
279     n=1000
280     dh=(Ptm-0)/n
281     sum=0.d0
282
283     do i=0,n
284         p=i*dh
285         f_p=(D(p))**4
286
287         if (i==0 .or. i==n) then
288             sum=sum+f_p
289         else
290             sum=sum+2*f_p
291         endif
292     end do
293     h=98.0665d0*(Ptm-0)*sum/(2*n)
294
295     End function
```

Subroutine Curves calculates for each generation (z=0-16) and for a specific range of transmural pressure (P_{tm}) the surface ratio (α):

```
296
297
298     Subroutine Curves
299     !*************************************************************************************************
300     !This subroutine re-creates the graphs of Lambert's model that describes the dependance of
301     !dimensionless parameter alpha α=A(Ptm)/Amax with transmural pressure.
302     !*************************************************************************************************
303
304     integer i
305     real*8 P,alfa
306
307     write(11,'("    Ptm \ Generation z:"\)')
308     do i=0,16
309         write(11,'(i10,\)') i
310     end do
311     write(11,*)
312
313     do P=-12,24,0.36
314         write(11,'(f9.4,18x," ",\)') P
315
316         do i=1,17
317             z=i-1
318             N_t=2.d0**z
319             L=T_L(i)                        ![=cm]
320             L=L*1.d-2                       ![=m]
321             a0=T_a0(i)
322             a0_=T_a0_(i)
323             n1=T_n1(i)
324             n2=T_n2(i)
325             Am=T_Am(i)                      ![=cm2]
326
327             Dmax=2.d0*dsqrt(Am/(N_t*pi))    ![=cm]
328             Dmax=Dmax*1.d-2                 ![=m]
329             P1=a0*n1/a0_
330             P2=-n2*(1-a0)/a0_
331
332             alfa=( D(P)/Dmax )**2
333             write(11,'(f7.4,2x" ",\)') alfa
334         end do
335
336         write(11,*)
337     end do
338
339     End subroutine
```

Subroutine Profile_1 calculates the variation of diameter D(x) and pressure P(x) along the cylindrical elastic tube using an iterative method:

```
340
341
342     Subroutine Profile_1
343     !*****************************************************************************************************
344     !This subroutine, for a pressure difference PtmA-PtmB across the tube that creates a flow rate Q,
345     !computes the profile of diameter D(x) and pressure Ptm(x) along the x-axis. For this purpose a
346     !numerical iterative method is required.
347     !*****************************************************************************************************
348     integer digits
349     real*8 Q_0, c, M
350
351     Q_0=Q
352     do digits=0,10
353         if (Q_0*(10**digits)>=1) exit
354     end do
355
356     write(20, '("P(A)=",f6.2," [kPa]",5x,"P(B)=",f6.2," [kPa]",6x,"Ppleural=",f6.2," [kPa]")')&
357     & P_A*98.0665d0/1000, P_B*98.0665d0/1000, P_pl*98.0665d0/1000
358     write(20, '("PtmA=",f6.2," [kPa]",5x,"PtmB=",f6.2," [kPa]",6x,"Q0=",f12.9," [L/s]")')&
359     & PtmA*98.0665d0/1000, PtmB*98.0665d0/1000, 1000*Q
360     write(20,*)
361     write(20,'("    x",10x,"P  (x)   u(x)     D(x)",7x,"Loops",7x,"Q(x)",9x,"Error",11x,"RE(x)",5x,"c(x)"),/')
362
363     sum1=0
364     x_nodes=100
365     dx=(L-0.d0)/x_nodes
366     x=dx
367     !Initial guess of Ptm(x) at A
368     PtmX=PtmA
369
370     do n=1,x_nodes
371
372         call PressureFlow(PtmA,PtmX,x)
373         diff=abs(Q-Q_0)
374         sum1=0
375         do while (diff>8.d-4/(10**digits))
376             sum1=sum1+1
377             if (Q<Q_0) then
378                 PtmX=PtmX-7.d-4
379             else
380                 PtmX=PtmX+7.1d-4
381             end if
382             call PressureFlow(PtmA,PtmX,x)
383             diff=abs(Q-Q_0)
384         end do
385
386         M=2*ro*dD(PtmX)/(98.0665d0*D(PtmX))
387         c=dsqrt(1.d0/M)
388
389         write(20,'(f9.6,2x,f9.4,2x,f6.3,2x,f9.6,2x,i8,2x,f13.9,2x,e14.8,4x,f6.1, 3x,f6.2)')&
390         & x, (PtmX+P_pl)*98.0665d0/1000, u_B, D_B, sum1, 1000*Q, diff, Re_B, c
391         print*, n, x, sum1
392         x=x+dx
393     end do
394
395     End subroutine
```

Subroutine Profile_2 calculates, also, the variation of diameter D(x) and pressure P(x) using a numerical method:

```
396
397
398     Subroutine Profile_2
399     !*************************************************************************************************
400     !This subroutine, for a pressure difference PtmA-PtmB across the tube that creates a flow rate Q,
401     !computes the profile of diameter D(x) and pressure Ptm(x) along the x-axis. In this algorithm, the
402     !profiles derive from an alternative equation (differantial form of Filoche's model), by solving
403     !numerically for the derivative dP/dx.
404     !*************************************************************************************************
405
406     integer n, P_nodes
407     real*8 Q_0, K, M, c, u, f, x, Ptm_ave, dP, dx, Ptm1, Ptm2, D_ave, Re
408
409     Q_0=Q                                          ![m3/s]
410     write(30,'("    x",10x,"P(x)",6x,"Ptm(x)",3x,"u(x)",6x,"D(x)",7x,&
411     &"RE(x)",2x,"u(x)/c(x)",2x,"c(x)",7x,"Q",5x,"Q_max"),/')
412
413     P_nodes=100
414     dP=(P_A-P_B)/P_nodes
415     x=0.d0
416     !Initial guess
417     Ptm1=PtmA
418     Ptm2=PtmA-dP
419
420     Re=4*ro*Q_0/(ita*pi*(D(Ptm1)))
421     u=4*Q_0/pi/(D(Ptm1)**2)                        ![m/s]
422     M=2*ro*dD(Ptm1)/(98.0665d0*D(Ptm1))
423     c=dsqrt(1.d0/M)
424     Q_max=c*pi*(D(Ptm2)**2)/4.d0
425
426     write(30,'(f9.6,2x,f9.4,2x,f9.4,2x,f6.3,2x,f9.6,4x,f6.1,3x,f6.4,3x,f6.2,2x,f8.6,2x,f8.6)')&
427     & x, (Ptm1+P_pl)*98.0665d0/1000, (Ptm1)*98.0665d0/1000, u, D(Ptm1), Re, u/c, c, 1000*Q, 1000*Q_max
428
429     do n=1,P_nodes
430
431         Ptm_ave=(Ptm1+Ptm2)/2.d0
432         D_ave=D(Ptm_ave)
433
434         Re=4*ro*Q_0/(ita*pi*(D_ave))
435
436         f=128*ita*Q_0*(alpha+beta*Re)/pi/(D_ave**4) ![Pa/m]
437         u=4*Q_0/pi/(D_ave**2)                       ![m/s]
438         M=2*ro*dD(Ptm_ave)/(98.0665d0*D_ave)
439         c=dsqrt(1.d0/M)                             ![m/s]
440
441         K=-f/ (1-((u/c)**2))/98.0665d0              ![cmH2O/m]
442         dx=-dP/K
443         x=x+dx
444         Q_max=c*pi*(D(Ptm2)**2)/4.d0
445
446         write(30,'(f9.6,2x,f9.4,2x,f9.4,2x,f6.3,2x,f9.6,4x,f6.1,3x,f6.4,3x,f6.2,2x,f8.6,2x,f8.6)')&
447         & x, (Ptm2+P_pl)*98.0665d0/1000, (Ptm2)*98.0665d0/1000, u,D(Ptm2),Re, u/c, c, 1000*Q, 1000*Q_max
448
449         Ptm1=Ptm2
450         Ptm2=Ptm2-dP
451     end do
452
453     End subroutine
```

Subroutine Prints write the results into the ‘’Result.txt’’ file:

```
454
455
456     Subroutine Prints
457     !*************************************************************************************************
458     !This subroutine compresses the typing proccess of the results.
459     !*************************************************************************************************
460
461     write(12,'(/,"-------INPUTS-------",/,"Generation z=",i2,/,"L=",f7.5," [m]")') z, L
462     write(12,'("Ptm(B)=",f11.2," [Pa]")') P_pl*98.0665d0
463     write(12,'("Ptm(A)=",f11.2," [Pa]")') PtmA*98.0665d0
464     write(12,'("Ptm(B)=",f11.2," [Pa]")') PtmB*98.0665d0
465     write(12,'("------RESULTS------")')
466     write(12,'("D(A)=",e9.3," [m]",/,"D(B)=",e9.3," [m]",/,"Dmax=",e9.3," [m]")') D_A, D_B, Dmax
467     write(12,'("Q=",f8.4," [l/s]")') 10**3*Q
468     write(12,'("Q_tot=",f8.4," [l/s]")') 10**3*Q*N_t
469     write(12,'("Ideal maximun flow rate (Poiseuille flow) through tube is:",/," Qmax  = ",f11.4,&
470     &" [l/s]",/," Q_Poiseuille  = ",f11.4," [l/s]")') 10**3*Qmax, 10**3*Q_Pois
471
472     End subroutine
473
474
475 End program
```